

## REE in suspended particulate matter and sediment of the Zuari estuary and adjacent shelf, western India: influence of mining and estuarine turbidity

R. Shynu, V. Purnachandra Rao\*, G. Parthiban, S. Balakrishnan<sup>§</sup>, Tanuja Narvekar and Pratima M. Kessarkar

CSIR-National Institute of Oceanography, Dona Paula-403004, Goa, India  
<sup>§</sup>Department of Earth Sciences, Pondicherry University, Pondicherry 605014, India

### ABSTRACT

Concentrations of Al, Fe, Mn and rare earth elements (REE) were measured in 122 samples of suspended particulate matter (SPM) and 70 surficial sediments from the Zuari estuary and the adjacent shelf to understand their distribution, provenance and estuarine processes. Concentrations of SPM were low in the upper estuary, increased seaward with high values in the lower estuary and then decreased at stations in the bay in all seasons. The distributions of mean  $\Sigma$ REE, Al and Fe along transect imitate each other and resemble inverted bowl-shaped pattern, with high and identical values at the lower estuary. The mean  $\Sigma$ REE, Al and Fe of sediment along transect showed two peak high values, one in the upper estuary and another in the bay amid low values corresponding to the lower estuary. The variations in the mean ratio of  $\Sigma$ REE<sub>SPM</sub>/ $\Sigma$ REE<sub>SED</sub> along transect resembled that of mean SPM at each station. The  $\Sigma$ REE of sediments in shallow shelf were close to that of the bay and, decreased seaward with increasing depth. PAAS-normalized REE patterns of every SPM/sediment sample revealed MREE- and HREE-enrichment with positive Ce and Eu anomalies. Ce/Ce\* was inversely correlated with Eu/Eu\* and salinity and, directly correlated with Mn concentrations. The results indicate that the REE of SPM/sediment is dominated by Fe, Mn ore dust and, its distribution along transect is controlled by the estuarine turbidity maximum (ETM). The ETM and seasonal circulation in the estuary controlled mixing and advective transport of particulates to the shelf during monsoon and, into the estuary during dry season. This study indicates sediment contribution to the shelf from tropical, minor rivers is controlled by hydrodynamic conditions in the estuaries and should not be underestimated.

Keywords: Rare earth elements, suspended matter, sediment, Zuari estuary, continental shelf, western India

---

\*Corresponding author. Tel.: 91-08322450 505; fax: 91-0832-2450 609

Email address: [vp rao@nio.org](mailto:vp rao@nio.org) (V. Purnachandra Rao)

## 1. Introduction

Rare earth elements (REE) form a key group of trace elements whose properties change systematically and gradually across the series (from La to Lu). Because of their coherent and predictable behavior, they have been used as geochemical tracers to characterize igneous rocks of various types, determine detrital sediment sources and elucidate seawater circulation patterns, hydrothermal fluxes and past oxygenation of the oceans (Piper, 1974; Henderson, 1984). The major sources of REE to the ocean are fluvial, atmospheric and hydrothermal vent exhalations (Elderfield and Greaves, 1982; Fleet, 1984). REE transported through fluvial source are extensively modified in the estuaries before reaching the ocean. Estuarine processes that affect the distribution of REE are flocculation, salt-induced coagulation of river organic colloids, adsorption-desorption reactions, remobilization due to early diagenetic changes and re-suspension (Hoyle et al., 1984). The behavior of REE in estuarine water and sediments across salinity gradient has been reported (Sholkovitz, 1976, 1993, 1995; Elderfield and Sholkovitz, 1987; Elderfield et al., 1990; Bau 1999; Chillou et al., 2006; Lawrence and Kamber, 2006; Censi et al., 2007; Marmolejo-Rodriguez et al., 2007). The distribution of REE in estuaries affected by acid mine drainage (Elbaz-Poulichet and Dupey, 1999; Johannesson and Zhou, 1999; Borrego et al., 2005) and geology of the hinterland (Prego et al., 2009, 2012) have also been reported. However, there are not many investigations on REE controlled by hydrodynamic conditions in the estuaries (Sholkovitz and Szymezak, 2000; Hannigan et al., 2010). Further, the studies on REE distribution in Indian estuaries are fewer, some examples being the Kavery River estuary (Ramesh et al., 1999; Singh and Rajamani, 2001) and Mandovi River estuary (Shynu et al., 2011). We report here the REE distribution in the Zuari River (ZR) estuary that is located a few kilometers south of the Mandovi River (MR) on the west coast of India (see Fig. 1A). Unlike MR, the main channel of Zuari River is dammed upstream and its seasonal discharge ( $147 \text{ m}^3 \text{ s}^{-1}$ ) into the estuary is much less than that of the MR ( $258 \text{ m}^3 \text{ s}^{-1}$ ). Because of the low seasonal river discharge and funnel-shaped bay off ZR one would expect greater impact of the tidal and wind-induced currents in defining estuarine processes and sediment distribution. The purpose of the paper is to report the distribution of REE in SPM and surface sediments of the Zuari estuary and adjacent shelf for the first time and, relate their distribution with sources and hydrodynamic conditions in the estuary.

## 2. Geological and estuarine settings of the Zuari River

The Zuari River (ZR) is a major river of Goa in the central west coast of India (Fig. 1A). It is ~50 km long and originates in the Western Ghats (mountain regions) and drains through a narrow coastal plain.

The main channel of ZR is connected to the Arabian Sea through a funnel-shaped, Mormugao Bay, which is ~10 km long, 5 m deep and has a maximum width of 5 km at its widest end (Fig. 1A). The ZR drains through rocks of Goa Group (Fig. 1B) belonging to the Dharwar Super Group of Archaean-Proterozoic age (Gokul et al., 1985). The basic rocks of Goa Group are green schists and gneisses and are largely covered by a residual weathered layer of rock (laterite), which is several tens of meters thick (Mascarenhas and Kalavampara, 2009). The original unweathered igneous and metamorphic rocks are, however, exposed only in coastal headlands or along steep slopes of high hill ranges. Sanvordem Formations (Fig. 1B) consisting of meta-greywacke, conglomerate and argillites occupy large area downstream of the Zuari River basin. The river runoff into the estuary is large in monsoon months and is regulated by a dam in the upper reaches (see Fig. 1A). The river runoff measured downstream of the dam during monsoon (June-September), post-monsoon (October- January) and pre-monsoon periods (February-May) are  $147 \text{ m}^3 \text{ s}^{-1}$ ,  $7.3 \text{ m}^3 \text{ s}^{-1}$  and  $0.8 \text{ m}^3 \text{ s}^{-1}$ , respectively (Rao et al., 2011). The estuary of the Zuari River is classified as a monsoonal, meso-tidal estuary. The tide ranges are ~2.3 m and 1.5 m during the spring and neap tides, respectively (Shetye et al., 2007). Tidal circulation dominates during dry period (October to May). Tidal oscillations have been observed and saline waters penetrate ~45 km upstream from the river mouth during dry period (Manoj and Unnikrishnan, 2009). Recent measurements of currents made in the estuary at Cortalim (station Z4, see Fig. 1A) show maximum values of longitudinal component of currents reach up to 80 cm/sec during spring tide (Dr. Unnikrishnan, personal communication) .

The Mandovi and Zuari (Ma-Zu) River estuaries are inter-connected through Cumbarjua canal close to their mouths (see Fig. 1A). Several big open cast iron and manganese (Fe-Mn) ore mines operate in the drainage basins of the Ma-Zu Rivers. The ores brought from mines are stored on the shores of the estuaries (Fig. 1C), loaded on to barges (Fig. 1C) at loading points and transported through the estuary to the port or mid-stream point, from where the ore is exported in giant ships. Of the 30.7 million tonnes (mt) of pulverized ore material transported in the year 2004 (Nagaraj and Raghuram, 2005), 19.1 mt of ore was transported through the MR and 11.6 mt was through ZR. About 11 mt of ore carried through the Mandovi was diverted to the port through Cumbarjua Canal and bay of Zuari during the monsoon.

### 3. Materials and methods

#### 3.1 Suspended particulate matter (SPM) sampling and chemical analyses

Two types of data were collected in the Zuari estuary during June 2008–May 2009: (1) Surface water was sampled every alternate day at one station (Z4) in the mid-channel of the estuary from June to September 2008. This station is referred to here as the “regular” station (Fig. 1A). (2) Surface water and bottom sediment were collected at stations along the main channel of the estuary every month during the spring tide. The stations are referred to as “transect” stations. Five liters of surface water sampled at each station were filtered through 0.4 µm polycarbonate membrane filter. Three Millipore filtration units (Model No. X104-220-50) were used simultaneously to filter 5 l of water at each station, i.e., each filtration unit takes about 1.7 l of water. De-ionized water was used to clean the filters. The SPM retained on filter papers was dried and weighted. SPM is expressed as milligram per liter. Salinity of surface water was invariably measured at all stations using conductivity sensor of a portable CTD system (Seabird SBE19 plus). The accuracy of the system for temperature and conductivity are 0.005° C and 0.0005 S/m, respectively.

A total of 122 samples of SPM were selected for determining the Al, Fe and Mn and, REE concentrations (Table 1A). This includes 16 samples from the regular station in addition, samples along transect stations. As we have sampled 6 stations (Z1 to Z6) during June–August, 8 stations (Z0 to Z7) in September and 10 stations (Z0 to Z9) during October–May, the total number of samples from transect stations are 106 (which can be summed up as: Z1–Z6:  $6 \times 3_{(\text{June-August})} + Z0\text{-Z7: } 8 \times 1_{\text{September}} + Z0\text{-Z9: } 10 \times 8_{(\text{October-May})} = \text{Total } 106 \text{ samples}$ ). The procedure for preparing SPM for chemical analysis is as follows: The SPM on the filter was carefully weighed and transferred to teflon beakers. The samples were digested using ultra pure acids with HF + HNO<sub>3</sub> + HClO<sub>4</sub> mixture in a beaker, kept overnight and then dried on a hot plate. This treatment was repeated till the sample in the beaker was completely digested. The final residue was dissolved in 20 ml of 1:1 HNO<sub>3</sub>. Subsequently, 5 ml of 1 ppm Rh solution was added as an internal standard and made up to the final volume (Govindaraju, 1994). These aliquots were analyzed for trace metals and REEs using Thermo X Series II Inductively-coupled plasma mass spectrometer (ICP-MS) at the National Institute of Oceanography, Goa, India. Major elements (Al, Fe and Mn) were analyzed using ICP-AES at the Department of Earth Sciences, Pondicherry University, India. MAG1 (Marine mud) was used as an internal standard to check the reliability of the analysis. Table 1B shows the certified values of major elements and rare earth elements of MAG 1 and values obtained in our experiments. The reproducibility of the results was

found to be better than 5% and 10% for major elements and REE, respectively. Table 2 shows the concentrations of major elements and REE in SPM at the regular station. Table 3 shows the average concentrations of major elements and REE in SPM at each station along with standard deviation (SD) on seasonal basis, i.e., the concentrations of elements at each station are obtained by averaging concentration values for four months - June to September (monsoon), October to January (post-monsoon) and February to May (pre-monsoon). The Ce (Ce/Ce\*) and Eu (Eu/Eu\*) anomalies were calculated, following Taylor and McLennan (1985).

### *3.2 Sediment sampling and chemical analyses*

Bottom sediment was collected along transect stations of the estuary, using Van Veen grab and the top centimeter of the surface sediment was carefully peeled off by opening one flap of the grab and dried. A total of 70 bottom sediment samples (50 from transect stations of the estuary and 20 from the continental shelf - Table 1A) were selected for chemical analyses. As we have chosen bottom sediments at 6 stations (Z1-Z6) each in August and September for monsoon period, 10 stations (Z0-Z9) each in November and December for post-monsoon and 10 stations (Z0-Z9) each in March and May for pre-monsoon, the total number of samples are  $52 (6 \times 2_{\text{August and September}} + 10 \times 2_{\text{November and December}} + 10 \times 2_{\text{March and May}})$ . The sediments at stations Z2 during monsoon and Z0 during pre-monsoon were sandy with < 9 % silt and 5 to 6% clay. Since we could not collect enough <2  $\mu\text{m}$  fraction of the sediment, these sediments were not analyzed. Therefore the number of samples at transect stations are 50. The <2  $\mu\text{m}$  fraction of the sediment was separated from the sediments using Stoke's settling velocity principle and dried. Following the aforementioned procedure the <2  $\mu\text{m}$  fraction of the sediment samples were digested and analyzed for major elements and REE concentrations. We have analyzed REE chemistry of the <2  $\mu\text{m}$  of sediments because (a) fine fraction includes colloids, and coagulation of colloids is a dominant process for removal of REE from the dissolved load in low salinity regions of estuaries (Sholkovitz, 1995). (b) Fine fraction records re-suspension of REE due to adsorption-desorption related to changes in salinity, pH and redox conditions (Hannigan et al., 2010) and allow us to explore the processes influencing estuarine sediment chemistry. Table 4 shows average concentrations of major elements and REE along with standard deviation (SD) in bottom sediments at each station on seasonal basis, i.e., the concentrations of elements at each station are obtained by averaging concentration values for two months - August and September for monsoon, November and December for post-monsoon and, March and May for pre-monsoon season.

## 4. Results

### 4. 1 Concentrations and composition of suspended matter

The concentrations of SPM at the regular station (RS) during monsoon varied between 3.3 mg/l and 68.6 mg/l while its total-REEs ( $\Sigma$ REE) varied between 111  $\mu$ g/g and 164  $\mu$ g/g (Table 2). The mean  $\Sigma$ REE ( $145.8 \pm 16.7$   $\mu$ g/g) was lower than the average SPM of World Rivers (174.8  $\mu$ g/g; Viers et al., 2009) and Post-Archaean average Australian Shale (PAAS: 184.8  $\mu$ g/g; McLennan, 1989).  $\Sigma$ REE increased with increase in SPM concentrations and, both were linearly correlated ( $r=0.64$ ;  $p<0.001$ ; Fig. 2A). Salinity of surface water at RS varied between 0 and 33 (Table 2). High concentrations of SPM and  $\Sigma$ REE were associated with low salinity as well as with high salinity water and, both showed no correlation with salinity (Fig. 2A). The Al, Fe and Mn concentrations of SPM ranged from 5.9-11.2%, 4.3-15.3% and 0.4-1.1%, respectively.  $\Sigma$ REE showed linear, positive correlation with Al and Fe ( $r=0.8$ ;  $p<0.001$ ) and no correlation with Mn (Fig. 2B). PAAS-normalized REE patterns showed MREE- and HREE-enrichment with positive Ce and Eu anomalies and exhibit no significant changes with variations in salinity or SPM concentrations.

Spatial and seasonal variations in the mean SPM,  $\Sigma$ REE, Al, Fe and Mn along transect stations and relationship of  $\Sigma$ REE with SPM and salinity are shown in Fig. 3A. Throughout the text the mean values of different parameters at each station given in Table 3 are presented and discussed. During monsoon the SPM concentrations were high at stations in the lower estuary and decreased seaward with increase in salinity at bay stations. During post- and pre-monsoons, the SPM was low in the upper estuary, except at station Z9 during post-monsoon, increased seaward in the lower estuary (Z6-Z3) and then decreased gradually in bay stations. Salinity increased seaward but showed no correlation with SPM in all seasons. Except at station Z7 during monsoon, the variations in  $\Sigma$ REE, Al and Fe along transect follow each other and resembled inverted bowl-shaped pattern, with high and near equal values at middle stations (Z3 to Z6) in all seasons (Fig. 3A). Mn decreased gradually from upper estuary to the bay in all seasons.  $\Sigma$ REE was directly correlated with SPM in all seasons but showed no correlation with salinity (Fig. 3A). PAAS-normalized REE showed MREE- and HREE-enriched patterns with positive Ce and Eu anomalies at every sample and season (Fig. 3B). The Ce anomaly ( $Ce/Ce^*$ ) values varied between 1.05 and 1.17, decreased seaward with near similar values at middle stations (Z3-Z7) during post- and pre-monsoons (Fig. 3B). The Eu anomaly ( $Eu/Eu^*$ ) varied between 1.27 and 1.68 with nearly identical values at landward stations (Z9 to Z4) and increased seaward at bay stations (Z3-Z0) during the monsoon and post-monsoon. During pre-monsoon  $Eu/Eu^*$  values were relatively

high in the lower estuary (Z7-Z4) and decreased away, either into the upper estuary (Z9-Z8) or bay (Z3 to Z0) (Fig. 3B). The normalized LREE to MREE ratio  $(L/M)_n$  showed a step-wise decreasing trend from upper estuary to the bay in all seasons (Fig. 3B). The normalized LREE to HREE ratio  $(L/H)_n$  decreased gradually seaward in the upper and lower estuary in all seasons.  $(L/H)_n$ , however, increased seaward in the bay during the monsoon and post-monsoon (Fig. 3B).

#### *4.2 Variations in REE of the sediments in the estuary and continental shelf*

Spatial variations in the mean  $\Sigma$ REE, Al, Fe and Mn of sediment in the estuary are shown in Fig. 4A. Throughout the text the mean values of different parameters at each station given in Table 4 are presented and discussed. The  $\Sigma$ REE of sediment ( $\Sigma$ REE<sub>SED</sub>) ranged between 175 and 320  $\mu$ g/g (Table 4) and was higher than in suspended particulate matter ( $\Sigma$ REE<sub>SPM</sub>: 89-169  $\mu$ g/g; Table 3). The variations in  $\Sigma$ REE<sub>SED</sub> along transect were opposite to that of  $\Sigma$ REE<sub>SPM</sub>. For example, the  $\Sigma$ REE<sub>SED</sub> along transect showed two peak high values, one in the upper estuary and another in the bay amid low values that correspond to the lower estuary in all seasons (Fig. 4A). The  $\Sigma$ REE<sub>SPM</sub> showed high values in the lower estuary and decreased values in the upper estuary and bay (Fig. 3A). The variations in the ratio of  $\Sigma$ REE<sub>SPM</sub> to  $\Sigma$ REE<sub>SED</sub> along transect, however, resembled that of SPM in each season (see Fig. 3A). The Fe of sediment increased and Mn decreased seaward during the monsoon. The distribution of Fe and Mn in sediments along transect, however, resembled that of  $\Sigma$ REE<sub>SED</sub> during the post- and pre-monsoons (Fig. 4A). Al distribution was similar to that of Fe during monsoon and pre-monsoon, with no significant trend along transect during the post-monsoon. PAAS-normalized REE patterns of sediment were similar to that of SPM with MREE- and HREE enrichment and positive Ce and Eu anomalies (Fig. 4A). The Ce/Ce\* and Eu/Eu\* values were higher in sediments (Table 4) than in suspended matter (Table 3). The distributions of Ce/Ce\*,  $(L/M)_n$  and  $(L/H)_n$  in sediments along transect resembled that of  $\Sigma$ REE in each season. The Eu/Eu\* showed a seaward increasing trend in all seasons (Fig. 4B).

The  $\Sigma$ REE of sediment on the continental shelf ranged from 62 to 190  $\mu$ g/g (Table 5) and decreased seaward with increasing depth.  $\Sigma$ REE showed linear correlation with Al ( $r=0.67$ ) and Fe ( $r=0.78$ ). The PAAS-normalized REE patterns (Fig. 5A) were similar to that of estuarine sediments. Ce/Ce\* (0.89-1.27) and Eu/Eu\* (1.38-1.64) values decreased with increasing depth, except the sediment at 11 m water depth which showed relatively low Ce/Ce\* (see Fig. 5A). Ce/Ce\* values showed moderate correlation with Mn concentrations (Fig. 5B).

The correlations of  $\Sigma\text{REE}$  with Al, Fe and Mn in SPM and sediment along transect stations are shown in Fig. 6. The  $\Sigma\text{REE}_{\text{SPM}}$  was linearly correlated with its Fe and Al during the monsoon and pre-monsoon and, moderately correlated during post-monsoon. It showed moderate correlation with Mn during the monsoon and post-monsoon. The  $\Sigma\text{REE}_{\text{SED}}$  however, showed no significant correlation with Al during monsoon and post-monsoon and, moderate correlation during pre-monsoon. The  $\Sigma\text{REE}_{\text{SED}}$ , however, showed strong to moderate correlation with Fe and Mn in all seasons.

## 5. Discussion

### 5.1 Occurrence of estuarine turbidity maximum in the lower estuary

The mean SPM concentrations increase seaward from upper estuary to the lower estuary and then decrease seaward in bay stations (Fig. 3A). High concentrations of SPM in the lower estuary are associated with low salinity surface water (1.4 to 9.8 between Z6 and Z3) during the monsoon and, with high salinity surface water (ranging from 17 to 33 between Z7 and Z3) during the post- and pre-monsoons. Higher SPM concentrations in the lower estuary than that of upper estuary and bay were discussed at length in Rao et al. (2011) and it was suggested that the estuarine turbidity maximum (ETM) played an important role in re-suspending bottom sediment and resulted in high SPM in the lower estuary. We investigate below the influence of ETM on REE distribution in the estuary.

### 5.2 Sources of REE in SPM during the monsoon (wet season)

Linear correlation of  $\Sigma\text{REE}$  with SPM, Al and Fe concentrations (Figs. 2, 3A and 6), indicate that the SPM dominated by clays (aluminosilicates) and Fe-rich particulates controlled the REE concentrations. Clays derived from the intense chemical weathering of hinterland formations and transported by the river and, Fe-particulates drained from ore deposits on the shore (Fig. 1C) could be the sources for REE. Smectite, kaolinite and goethite occur in SPM of the Zuari during monsoon (Kessarkar et al., 2013). Coppin et al. (2002) reported strong REE sorption on smectite because of permanent negative charge and, pH dependent REE sorption on kaolinite. Dissolved, colloidal and particulate Fe-Mn oxyhydroxides are expected to be flushed into the estuary from ore deposits (Fig. 1C) during heavy monsoon rains. Since REE have strong affinity to co-precipitate and adsorb on to Fe-Mn oxyhydroxides, (Elderfield et al., 1990; Andersson et al., 2005 and Marmolejo-Rodriguez et al., 2007), the dissolved and colloidal REE may have scavenged/adsorbed onto the surfaces of Fe-O-OH and  $\text{MnO}_2$  and clay minerals at low salinities, then coagulated and transferred into the particulate form. Several investigators reported large scale removal of dissolved, colloidal and particulate REEs in low



salinity (<5) water zone of estuaries (Hoyle et al., 1984; Elderfield et al., 1990; Sholkovitz, 1993). In this study  $\Sigma$ REE showed no correlation with salinity (Figs. 2A and 3A). Despite low salinities at stations (Z7 to Z3) in the lower estuary, the SPM,  $\Sigma$ REE, Al and Fe concentrations are high and,  $\Sigma$ REE, Al and Fe values are similar at Z3 to Z5 (Fig. 3A; Table 3). This may be due to the occurrence of estuarine turbidity maximum (ETM). During monsoon the river flow is countered by the tidal and monsoon wind-induced currents and results in the development of ETM in the lower estuary (Rao et al., 2011). As a consequence bottom sediment may have been re-suspended, thereby increasing SPM and REE in the water column and mixed up with the sediment brought by the river. In other words, the REE variations induced by salinity changes along transect are overprinted by REE associated with re-suspended particulates and, therefore no significant changes in  $\Sigma$ REE, Al and Fe concentrations are observed (Fig. 3A). Although the concentrations of these elements show a decreasing trend at bay stations (Fig. 3A), the mean Al values in SPM remain similar in the upper estuary (10.7), lower estuary ( $10.8 \pm 1.1$ ) and bay ( $10.0 \pm 0.9$ ). This suggests strong influence of turbidity maximum even in the bay

### *5.3 Sources of REE in SPM during the post- and pre-monsoons (dry season)*

The mean concentrations of SPM and its  $\Sigma$ REE, Fe, and Al during the post- and pre-monsoons are lower in the upper estuary than in lower estuary (Fig. 3A). In other words, high SPM at middle stations (see Fig. 3A) largely coincide with inverted bowl-shaped pattern of  $\Sigma$ REE, Fe, and Al in the lower estuary. Moreover,  $\Sigma$ REE showed moderate to strong correlation with SPM (Fig. 3A), Fe and Al (Fig. 6) during dry season. Since river discharge is low during dry season, the seaward increase of SPM was attributed to the estuarine turbidity maximum (ETM; Rao et al., 2011), which is controlled by the tidal and offshore wind-induced currents and funnel-shaped bay off Zuari; the latter may have been effective in magnifying the energy and effectiveness of the tidal and wind-induced currents as they propagate towards the narrower part of the funnel-shaped bay and made a greater impact on the erosion and re-suspension of material. Thus the geometry of the bay and seasonal currents played major roles in re-suspending bottom sediments and contributed high SPM,  $\Sigma$ REE, Fe and Al in the lower estuary. Elderfield et al. (1990) reported REE maximum associated with turbidity maximum in the Delaware estuary. As Z9 is an ore handling station, high Fe and Mn at Z9 (see Fig. 3A) indicate ore dust fallen into the estuary may have locally influenced their concentrations (see Fig. 1C). Though the concentrations of SPM vary at each station, the  $\Sigma$ REE, Fe and Al values are high and identical at middle stations (Z3-Z7; Fig. 3A). This may indicate advective transport of re-suspended fine-grained particulates of SPM by existing currents and homogenization of the concentrations of elements in the

SPM. Advective transport affecting the metal and nutrient distribution was reported in small, narrow estuaries such as Waquoit and the Fly/Gulf of Papua (Huettel et al., 1998; Charette et al., 2005). Tidal circulation dominates during dry season. Manoj and Unnikrishnan (2009) reported tidal oscillations and seawater as far as ~45 km upstream from the mouth of Zuari during dry season. The homogenized values of  $\Sigma\text{REE}$ , Fe and Al at stations in the lower estuary may therefore reflect influence of tidal and wind-induced currents in re-suspending bottom sediments and advective transport of particulates upstream.

#### *5.4 Relationship of $\Sigma\text{REE}$ in sediment and SPM*

The distribution of  $\Sigma\text{REE}_{\text{SED}}$  along transect is simply opposite to that of  $\Sigma\text{REE}_{\text{SPM}}$ . Since the sediments with relatively low  $\Sigma\text{REE}$  (Fig. 4A) correspond to SPM with high  $\Sigma\text{REE}$  in the lower estuary (Fig. 3A) it could be that the bottom sediments in lower estuary were re-suspended into the water column, thereby increasing sediment particulates (SPM) and associated REE. The variations in the mean ratio of  $\Sigma\text{REE}_{\text{SPM}}$  to  $\Sigma\text{REE}_{\text{SED}}$  resemble that of mean SPM at each station (see Fig. 3A) implying particulates re-suspended from bottom sediment by ETM are indeed responsible for high SPM and  $\Sigma\text{REE}$  in the lower estuary. In other words, ETM played a major role for the coupling of  $\Sigma\text{REE}$  of sediment and SPM.

During monsoon the Al and  $\Sigma\text{REE}$  of suspended matter are positively correlated. The Al concentrations of sediments are, however, high (Table 4), showed no correlation with  $\Sigma\text{REE}$  during monsoon and post-monsoon and moderate correlation during pre-monsoon (Fig. 6). The Fe and Mn of sediment, however, showed moderate to strong correlation with  $\Sigma\text{REE}$  in all seasons (Fig. 6). It may be because of the turbidity maximum, the REE associated with lighter, aluminosilicates (clay minerals) were repeatedly re-suspended and the adsorbed REE are stripped off and transported further, while REE associated with heavy, Fe, Mn particulates are retained largely in sediments. In other words, the REE of sediments may largely be due to particulate Fe and Mn oxyhydroxides from ore deposits (see below). The values of  $\Sigma\text{REE}$  of sediment at shallow shelf (180-189  $\mu\text{g/g}$  at 7 m; Table 5) are close to that of the mean  $\Sigma\text{REE}$  of bay (195.5  $\mu\text{g/g}$ ). Moreover,  $\Sigma\text{REE}$  showed linear correlation with Al and Fe implying that the clays and Fe-oxyhydroxides contributed REE to the shelf region.

#### *5.5 PAAS-normalized REE patterns in SPM and sediment*

MREE- and HREE enriched REE patterns with positive Ce and Eu anomalies are characteristic of both SPM and sediment (Figs. 3A, 4A and 5). They are different from that of the upper continental crust

(Taylor and McLennan, 1985) and SPM of major World Rivers (Goldstein and Jacobson, 1988) which show LREE enriched patterns. Since the REE patterns are consistent in all SPM/sediment samples and in all seasons, they may reflect the composition of the dominant detrital material delivered to the estuary/shelf. The MREE- and HREE-enriched REE patterns with positive Ce and Eu anomalies were reported in the pre-cambrian metamorphic rocks (Fig. 1B; Dhoundial et al., 1987; Naqvi 2005; Desai et al., 2009). As parent rocks are covered by thick laterites (Mascarenhas and Kalavampara, 2009) they may not be the major source of REE in the estuary. Moreover, REE patterns of SPM/sediment do not vary in dry season (Fig. 4A, 5A and 6) when river discharge into the estuary was negligible. This implies that the clays transported by the Zuari River may not be dominantly influencing the composition of REE. As ore handling is active at shore stations throughout the year (Fig. 1C), ore particulates flushed into the estuary during heavy monsoon rains and ore dust spilled over into the estuary while transferring ore into barges or, transporting ore to the port through the estuary may act as dominant source for REE. Strong resemblance of REE patterns of Fe-Mn ores (Fig. 3A) with that of SPM / sediment in Zuari estuary attests that the ore dust controlled REE composition.

#### *5.6 Ce anomaly in SPM and sediment*

$Ce^{3+}$  oxidizes to less soluble  $Ce^{4+}$  in estuarine and marine water and is rapidly removed to the sediment by particle scavenging. As a consequence one would expect negative Ce anomaly in estuarine/seawater and positive Ce anomaly in sediment below. Since positive Ce anomaly is characteristic of every sample of SPM/sediment it must have been inherited from ore dust transferred to the estuary from time to time. Positive Ce anomaly is a characteristic of Fe, Mn-oxide particulates (De Carlo et al., 1998; Bau, 1999; Tachikawa et al., 1999; Ohta and Kawabe, 2001). The variations in  $Ce/Ce^*$  (Figs. 3B and 4B) along transect may indicate response of total Ce (dissolved, colloidal and particulate) to the estuarine conditions.  $Ce/Ce^*$  negatively correlates with salinity (Fig. 7A). The  $Ce/Ce^*$  in suspended matter decreased sharply at low (<10) salinities in the upper estuary, maintained similar values at stations in the lower estuary and then decreased seaward at bay stations during the post- and pre-monsoons (see Fig. 3B). Ce is one among the LREE. As the initial decrease in  $Ce/Ce^*$  is accompanied by decrease in  $(L/H)_n$  at low salinities (Fig. 3B), salinity-induced coagulation of river colloids and fractionation among REEs may have been involved. Sholkovitz (1993) reported preferential removal of LREE at low salinity region. The behavior of  $Ce/Ce^*$  is same as that of  $\Sigma REE$  in the lower estuary and both showed high, near identical values at stations Z3 to Z6 (Fig. 3B). This indicates that the  $Ce/Ce^*$  values, similar to  $\Sigma REE$ , are influenced by ETM.  $Ce/Ce^*$  decreases seaward at bay stations during the post- and pre-monsoons (Fig. 3B). Pednekar et al. (2011) reported increased productivity in

the estuary, immediately after the monsoon. The decrease of Ce/Ce\* could be due to biologically mediated oxidation of Ce<sup>3+</sup> to Ce<sup>4+</sup> and scavenging of Ce<sup>4+</sup> to the sediments. Sholkovitz (1993) showed a two step decrease of Ce/Ce\* in the Amazon estuary, one in low salinity zone and another in the zone of high biological productivity. Ce and Mn are redox-sensitive elements and their distributions are expected to be governed by similar mechanisms. Although Ce/Ce\* is linearly correlated with Mn (Fig. 7B), Mn concentrations decreased more rapidly seaward (Fig. 3A), whereas Ce/Ce\* showed elevated and equal values at middle stations during dry season (Fig. 3B). It appears that the Ce is more sensitive to physical mixing than that of Mn. Hannigan et al. (2010) suggested oxidation and slight changes in physical mixing and particle settling lead to differences in Ce/Ce\* value.

The distributions of Ce/Ce\* value, Mn concentrations and  $\Sigma$ REE of sediments along transect resemble each other (Figs. 4A-B) and are relatively depleted in the lower estuary implying that the hydrodynamic conditions at the intersection of bay and lower estuary favoured erosion and re-suspension of bottom sediments. Ce/Ce\* decreases with increasing depth in the shelf sediments and is linearly correlated with Mn (Fig. 5A-B). The low Ce/Ce\* (0.89) in sediment collected at 200 m in the oxygen minimum zone (OMZ; 150-1000 m; Sengupta and Naqvi, 1984) may be due to the reduction Ce<sup>4+</sup> to Ce<sup>3+</sup> at the sediment-water interface or during early diagenesis of organic-rich, sediments and then diffusion of Ce<sup>3+</sup> into the water column.

#### 5.7. *Eu anomaly (Eu/Eu\*) in SPM and sediment*

Positive Eu/Eu\*, similar to Ce/Ce\*, is characteristic of every SPM/sediment sample (Fig. 3B, 4B and 5A) suggesting that it also may have inherited from ore dust. Positive Eu/Eu\* in sediments of Vigo Ria (Prego et al., 2009) and, SPM/sediment of the Mandovi estuary (Shynu et al., 2011) were attributed to sediment-parent material. Eu/Eu\* shows negative correlation with Ce/Ce\* (Fig. 7D). The Eu/Eu\* values in suspended matter increased seaward at bay stations and decoupled with Ce/Ce\* during monsoon and post-monsoon (Fig. 3B). Hannigan et al. (2010) suggested that decoupling of Ce and Eu anomalies could be due to the slow dissolution rate of Eu-humate complexes, differences in complexation behavior of Eu relative to other REE, and the presence of allochthonous adsorbed Eu. Eu is more stable in seawater and the rate of removal of Eu is less than the other REE (Nozaki et al., 2000). Increase in Eu/Eu\* is associated with decrease in (L/M)<sub>n</sub> (Fig. 3B) and (H/M)<sub>n</sub> (Table 3) at bay stations; this suggests an overall enrichment of MREE during monsoon and post-monsoon. Since ore dust is MREE and HREE-enriched, it is likely that the bay received more dust during this period. Nagaraj and Raghuram (2005) reported that a part of the ore carried through the Mandovi estuary is diverted to the

port through Cumbarjua canal (see Fig. 1A) during monsoon; this suggest that the bay off Zuari indeed experiences increased barge traffic carrying ore during monsoon, i.e., ore carried through the Zuari estuary and, the traffic that is from Mandovi. As ore is reloaded into giant ships at the port, located in the bay (Fig. 1A), one would expect increased spillage of ore dust into the bay. In other words, increased supply of ore dust to the bay water may have resulted in increased Eu anomaly. During the pre-monsoon  $\text{Eu}/\text{Eu}^*$  decreases with increase in  $(\text{L}/\text{M})_n$  (Fig. 3B) and  $(\text{H}/\text{M})_n$  (Table 3). As productivity is high at bay stations during dry season, coatings of organic matter and Fe-Mn oxides may have scavenged REE to the sediments.  $\text{Eu}/\text{Eu}^*$  in SPM is therefore controlled by supply of ore dust and biological productivity at different times at bay stations.

## 6 Conclusions

The distribution of REE was investigated in 122 samples of suspended matter and 70 sediments of the Zuari estuary and adjacent shelf. The SPM,  $\Sigma\text{REE}$ , Fe and Al concentrations in SPM are high in the lower estuary but low in the upper estuary and bay in all seasons suggesting estuarine turbidity maximum (ETM) played an important role in lateral variations of SPM and its elemental concentrations. The positive correlation of  $\Sigma\text{REE}$  with its Al, Fe and Mn in SPM indicates clays and Fe-Mn particulates contributed REE. The sediment with relatively low  $\Sigma\text{REE}$  corresponding to SPM with high  $\Sigma\text{REE}$  in the lower estuary indicate coupling between SPM and sediment and, the role of ETM in re-suspending bottom sediments. MREE- and HREE-enriched patterns with positive Ce and Eu anomalies in every sample of SPM/sediment suggest that REE are largely contributed by Fe-Mn ore dust.  $\text{Ce}/\text{Ce}^*$  and Mn concentrations in SPM are linearly correlated with each other but negatively correlated with salinity.  $\text{Eu}/\text{Eu}^*$  in SPM is largely controlled by supply of ore dust and biological productivity. We suggest that REE of SPM/sediment in the Zuari estuary are dominated by ore dust and their distribution along transect of the estuary is controlled by hydrodynamic conditions. Despite Zuari is a minor river with low discharge into the estuary, significant REE are transported to the continental shelf, suggesting that the detrital supply from tropical, minor rivers should not be underestimated.

## Acknowledgements

We thank the Director, National Institute of Oceanography, Goa for facilities. Research fellowship for R. Shynu and Tanuja Narvekar was supported by Project funds from the Ministry of Earth Sciences (GAP 2002) and Supra-institutional Project (SIP 1008), respectively. We thank Mr. R. Uchil for drawing the 'Geology of Goa'. We thank John T. Wells, Editor and the anonymous reviewers of Marine Geology for their critical comments on the manuscript. This is NIO contribution

## References

- Andersson, K., Dahlgvist, R., Turner, D., Stolpe, B., Larsson, T., Ingri, J., Andersson, P., 2005. Colloidal rare earth elements in a boreal river: changing sources and distributions during the spring flood. *Geochimica et Cosmochimica Acta* 70, 3261-3274.
- Bau, M., 1999. Scavenging of yttrium and rare earths by precipitating iron oxyhydroxide: experimental evidence for Ce oxidation, Y-Ho fractionation and lanthanide tetrad effect. *Geochimica et Cosmochimica Acta* 63, 67-77.
- Borrego, J., López-González, N., Carro, B., Lozano-Soria, O., 2005. Geochemistry of rare-earth elements in Holocene sediments of an acidic estuary: environmental markers (Tinto River estuary, South-western Spain). *Journal of Geochemical Exploration* 86, 119-129.
- Censi, P., Sprovieri, M., Saiano, F., Di Geronimo, S.I., Larocca, D., Placenti, F., 2007. The behaviour of REEs in Thailand's Mae Klong estuary: suggestions from the Y/Ho ratios and lanthanide tetrad effects. *Estuarine, Coastal and Shelf Science* 71, 569-579.
- Chillou, G., Anschutz, P., Lavaux, G., Blane, G., 2006. Rare earth elements in the modern sediments of the Bay of Biscaye (France). *Marine Chemistry* 100, 39-52.
- Charette, M.A., Sholkovitz, E.R., Hansel, C.M., 2005. Trace element cycling in a subterranean estuary: Part 1 Geochemistry of the permeable sediments. *Geochimica et Cosmochimica Acta* 69, 2095-2100.
- Coppin, F., Berger, G., Bauer, A., Caslet, S., Loubet, M., 2002. Sorption of lanthanides on smectite and kaolinite. *Chemical Geology* 182, 57-68.
- De Carlo, E., Wen, X.Y., Irving, M., 1998. The influence of redox reactions on the uptake of dissolved Ce by suspended Fe and Mn oxide particles. *Aquatic Geochemistry* 3, 357-389.
- Desai, A.G., Arolkar, D.B., French, D., Viegas, A., Vishwanath, T.A., 2009. Petrogenesis of the Bondla layered mafic-ultramafic complex Usgaon, Goa. *Journal of Geological Society of India* 73, 697-714.
- Dhondial, D.P., Paul, D.K., Sarkar, A., Trivedi, J.R., Gopalan, K., Potts, P.J., 1987. Geochronology and geochemistry of the Precambrian granitic rocks of Goa, SW India. *Precambrian Research* 36, 287-302.
- Elbaz-Poulichet, E., Dupey, C., 1999. Behavior of rare earth elements at the freshwater-seawater interface of two acid mine riversL the Tinto and Odiel (Andalucia, Spain). *Applied Geochemistry* 14, 1063-1072.
- Elderfield, H., Greaves, M.J., 1982. The rare earth elements in seawater. *Nature* 296, 214-219.
- Elderfield, H., Sholkovitz, E.R., 1987. Rare earth elements in porewater of reducing nearshore sediments. *Earth and Planetary Science Letters* 82, 280-288.

- Elderfield, H., Upstill-Goodard, R., Sholkovitz, E.R., 1990. The rare earth elements in rivers, estuaries and coastal seas and their significance to the composition of seawater. *Geochimica et Cosmochimica Acta* 54, 971-991.
- Fleet, A.J., 1984. Aqueous and sedimentary geochemistry of the rare earth elements In: Henderson, P. (ed.) *Rare Earth Elements Geochemistry*, Elsevier, Amsterdam, pp. 343-373.
- Gokul, A.R., Srinivasan, M.D., Gopalakrishnan, K., Viswanathan, L.S., 1985. Stratigraphy and Structure of Goa. Seminar Volume on Earth Resources for Goa's Development. Geological Survey of India, pp. 1-13.
- Goldstein, S.J., Jacobsen, S.B., 1988. Rare earth elements in river waters. *Earth Planetary Science Letters* 89, 35-47.
- Govindaraju, K., 1994. Compilation of Working Values and Sample Description for 383 Geostandards, vol. 18. *Geostandard Newsletter (Special issue)* 158 pp.
- Hannigan, R., Dorval, E., Jones, C., 2010. The rare earth element chemistry of estuarine surface sediments in the Chesapeake Bay. *Chemical Geology* 272, 20-30.
- Henderson, P., 1984. Rare earth element Geochemistry, Elsevier Amsterdam  
 Hoyle, J., Elderfield, H., Gledhill, A., Greaves, M., 1984. The behaviour of rare earth elements during mixing of river and sea waters. *Geochimica et Cosmochimica Acta* 48, 143-149.
- Hoyle, J., Elderfield, H., Gledhill, A., Greaves, M., 1984. The behaviour of rare earth elements during mixing of river and sea waters. *Geochimica et Cosmochimica Acta* 48, 143-149.
- Huettel, M., Ziebis, W., Forster, S., Luther, G.W., 1998. Advective transport affecting metal and nutrient distribution and interfacial fluxes in permeable sediments. *Geochimica et Cosmochimica Acta* 62, 613-631.
- Kessarkar, P.M., Shynu, R., Rao, V.P., Feng Chong, Narvekar, T and Zhang, J., 2013. Geochemistry of the suspended sediment in the estuaries of the Mandovi and Zuari Rivers, Central west coast of India. *Environmental Monitoring and Assessment* 185, 4461-4480.
- Johannesson, K.H., Zhou, X., 1999. Origin of middle rare earth elements enrichments in acid waters of a Canadian High Arctic lake. *Geochimica et Cosmochimica Acta* 61, 153-165.
- Lawrence, M.G., Kamber, B.S., 2006. The behavior of the rare earth elements during estuarine mixing – revised. *Marine Chemistry* 100, 147-161.
- Manoj, N.T., Unnikrishnan, A.S., 2009. Tidal circulation and salinity distribution in the Mandovi and Zuari estuaries: case study. *Journal of Waterway, Port, Coastal and Ocean Engineering* 135: 278-287.
- Marmolejo-Rodríguez, A.J., Prego, R., Meyer-Willerer, A., Shumilin, E., Sapozhnikov, D., 2007. Rare earth elements in iron oxy\_hydroxide rich sediments from the Marabasco River-Estuary System

(Pacific coast of Mexico), REE affinity with iron and aluminium. *Journal of Geochemical Exploration* 94, 43-51.

Mascarenhas, A. and Kalavampara, G., 2009. Natural resources of Goa: A geological perspective. Geological Society of Goa, Miramar, Goa. 213 p.

McLennan, S.M., 1989. Rare earth elements in sedimentary rocks: influence of provenance and sedimentary processes. In: Lipin, B.R., Mckay, G.A. (Eds.), *Geochemistry and Mineralogy of Rare Earth Elements*. *Reviews in Mineralogy* 21, pp. 169-200.

Nagaraj, J.N., Raghuram, G., 2005. Viability of inland water transport in India – A report . Presented at Workshop 'Strengthening Policy Reforms for Transport Development in India', sponsored by Asian Development Bank and Department of Economic Affairs, Delhi, 35 p.

Naqvi, S.M., 2005. Geology and evolution of the Indian Plate (from Hadean to Holocene (4 Ga to 4 Ka). Capital publishing company, New Delhi, p. 450.

Nozaki, Y., Lerche, D., Sotto, A.D., Snidvongs, A., 2000. The estuarine geochemistry of rare earth elements and Indium in the Chao Phraya River, Thailand. *Geochimica et Cosmochimica Acta* 64, 3983-3994.

Ohta, A., Kawabe, I., 2001. REE (III) adsorption onto Mn dioxide and oxyhydroxide: Ce(III) oxidation by delta MnO<sub>2</sub>. *Geochimica et Cosmochimica Acta* 65, 695-703.

Pednekar, S., Matondkar, S.G.P., Gomes, H.D.R., Goes, J.I., Parab, S., Kerkar, V., 2011. Fine-scale responses of phytoplankton to freshwater influx in a tropical monsoonal estuary following the onset of southwest monsoon. *Journal of Earth System Science* 120, 545-556.

Piper, D.Z., 1974. Rare earth elements in the sedimentary cycle: a summery. *Chemical Geology* 14, 285-315.

Prego, R., Caetano, M., Vale, C., Marmolejo-Rodriguez, J., 2009. Rare earth elements in sediments of the Vigo Ria, NW Iberian Peninsula. *Continental Shelf Research* 29, 896-902.

Prego, R., Caetano, M., Bernardez, P., Brito, P., Ospina-Alvarez, N., Vale, C., 2012. Rare earth elements in coastal sediments of the norther Galician shelf: Influence of geological features. *Continental Shelf Research* 35, 75-85.

Ramesh, R., Ramanathan, A.L., Arthur James, R., Subramanian, V., Jacobsen, S.B., Holland, H.D., 1999. Rare earth elements and heavy metal distribution in estuarine sediments of east coast of India. *Hydrobiologia* 57, 1-11.

Rao, V.P., Shynu, R., Kessarkar, P.M., Sundar, D., Michael, G.S., Narvekar, T., Blossom, V., Mehra, P., 2011. Suspended sediment dynamics on a seasonal scale in the Mandovi and Zuari estuaries, Central west coast of India. *Estuarine. Coastal and Shelf Science* 91, 78-86.

Rollinson, H., 1993. Using trace elements data. In: Rollinson, H. (Ed.), *Using geochemical data: evaluation, presentation, interpretation*. Pearson, Prentice Hall, pp. 133-134.



- Sen Gupta, R., Naqvi, S.W.A., 1984. Chemical oceanography of the Indian Ocean, north of Equator. *Deep-Sea Research* 31, 671-707.
- Shetye, S.R., Kumar, M.D., Shankar, D., 2007. The Mandovi and Zuari estuaries. National Institute of Oceanography, Goa, 145 pp.
- Sholkovitz, E.R., 1976. Flocculation of dissolved organic and inorganic matter during the mixing of river water and seawater. *Geochimica et Cosmochimica Acta* 40, 831-845.
- Sholkovitz, E.R., 1993. The geochemistry of rare earth elements in the Amazon River estuary. *Geochimica et Cosmochimica Acta* 57, 2181-2190.
- Sholkovitz, E.R., 1995. The aquatic chemistry of rare earth elements in rivers and estuaries. *Aquatic Geochemistry* 1, 1-34.
- Sholkovitz, E., Szymezak, R., 2000. The estuarine chemistry of rare earth elements: comparison of the Amazon, Fly, Sepik and Gulf of Papua systems. *Earth and Planetary Science Letters* 178, 299-309.
- Shynu, R., Rao, V.P., Kessarkar, P.M., Rao, T.G., 2011. Rare earth elements in suspended and bottom sediments of the Mandovi estuary, central west coast of India: Influence of mining. *Estuarine, Coastal and Shelf Science* 94, 355-368.
- Singh, P., Rajamani, V., 2001. Geochemistry of the floodplain sediments of the Kaveri river, Southern India. *Journal of Sedimentary Research* 71, 50-60.
- Tachikawa, K., Jeandel, C., Vangriesheim, A., Dupre', B., 1999. Distribution of rare earth elements and neodymium isotopes in suspended particles of the tropical Atlantic Ocean (EUMELI site). *Deep Sea Research* 46, 733-756.
- Taylor, S.R., McLennan, S.M., 1985. *The Continental Crust: Its Composition and Evolution*. Blackwell, Oxford, p. 312.
- Viers, J., Dupre, B., Gaillardet, J., 2009. Chemical composition of suspended sediments in world rivers: new insights from a new database. *Science of the Total Environment* 407, 853-868.

## Figure captions

- Fig. 1. (A) Location of sample stations in the Zuari River estuary and adjacent shelf, west coast of India. Insert Figure shows the location of sample stations on the continental shelf. (B) Geology of the Zuari river basin (modified after Mascarenhas and Kalavampara, 2009) and (C) Photographs showing Fe, Mn ore deposits stored on the shore of the Zuari estuary (left) and, loading of Fe, Mn ores into barges (right).
- Fig. 2. Relationship of  $\Sigma\text{REE}$  with SPM concentrations and salinity (A), and with Al, Fe and Mn concentrations (B) of SPM at the regular station.
- Fig. 3A. Distributions of mean SPM, salinity and ratio of  $\Sigma\text{REE}_{\text{SPM}}/\Sigma\text{REE}_{\text{SED}}$  (left column), mean  $\Sigma\text{REE}$ , Al, Fe and Mn of SPM (middle column) along transect stations of the Zuari estuary during the monsoon, post- and pre-monsoons. The relationship of  $\Sigma\text{REE}$  with SPM and salinity is also shown in the right column. Shadow in the left and middle columns marks the stations in the lower estuary and enables to distinguish the stations in the upper estuary and bay.
- Fig. 3B. PAAS-normalized REE patterns of suspended matter (left column), distribution of mean Ce/Ce\* and Eu/Eu\* (middle column) and, normalized mean (L/H)<sub>n</sub> and (L/M)<sub>n</sub> values (right column) along transect stations of the estuary during the monsoon, post- and pre-monsoons. PAAS-normalized REE pattern of ore deposits is also shown. Shadow in the middle and right columns marks the stations in the lower estuary and enables to distinguish the stations in the upper estuary and bay.
- Fig. 4A. Distribution of  $\Sigma\text{REE}$ , Al, Fe and Mn (left column) and PAAS-normalized REE patterns (right column) in sediments along transect stations of the estuary during the monsoon, post- and pre-monsoons. Shadow in the left column marks the stations in the lower estuary and enables to distinguish the stations in the upper estuary and bay.
- Fig. 4B. Distribution of mean Ce/Ce\* and Eu/Eu\* (left column) and, normalized mean (L/H)<sub>n</sub> and (L/M)<sub>n</sub> (right column) in sediments along transect stations during the monsoon, post- and pre-monsoons. Shadow in the left and right columns marks the stations in the lower estuary and enables to distinguish the stations in the upper estuary and bay.
- Fig. 5. PAAS-normalized REE patterns (A) and, relationship of Ce/Ce\* values with Mn concentrations (B) in sediments from the continental shelf.
- Fig. 6. Relationship of  $\Sigma\text{REE}$  with Al, Fe and Mn in SPM and sediments during the monsoon, post- and pre-monsoons.
- Fig. 7. Relationship of Ce/Ce\* with salinity (A), and Mn concentrations (B) in SPM. A plot between Ce/Ce\* and Mn concentrations of sediments (C) and, Ce/Ce\* and Eu/Eu\* in SPM (D) are also shown.

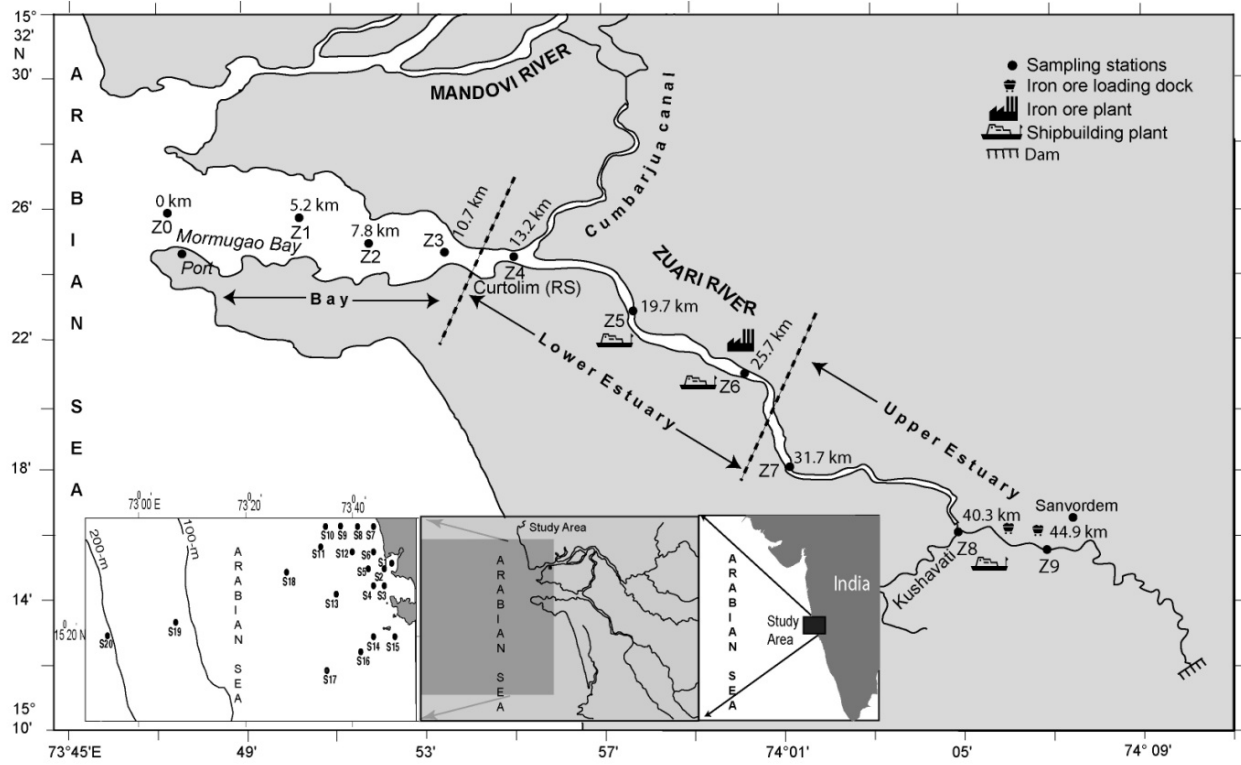


Fig. 1 A

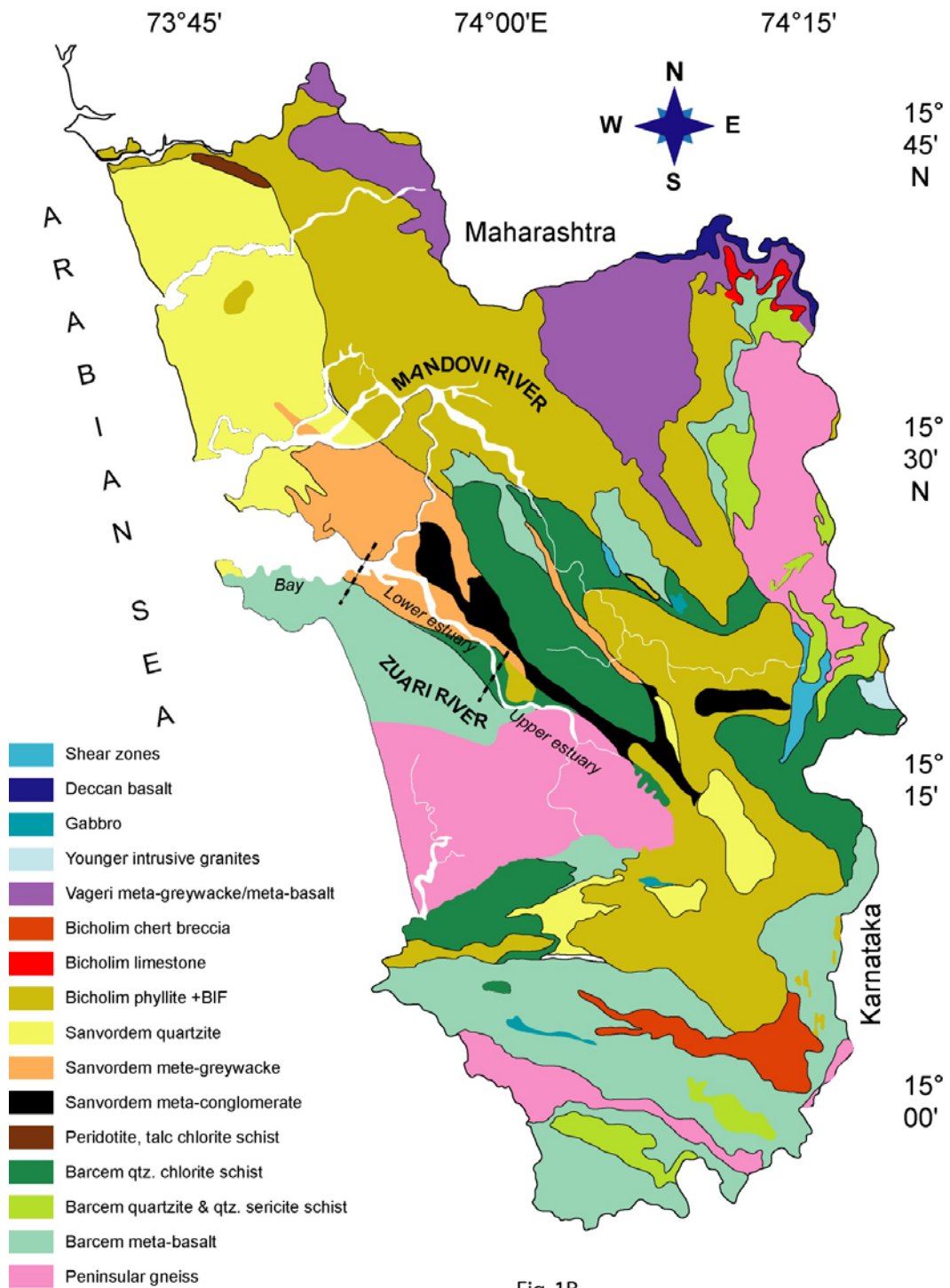


Fig. 1B



Fig. 1C

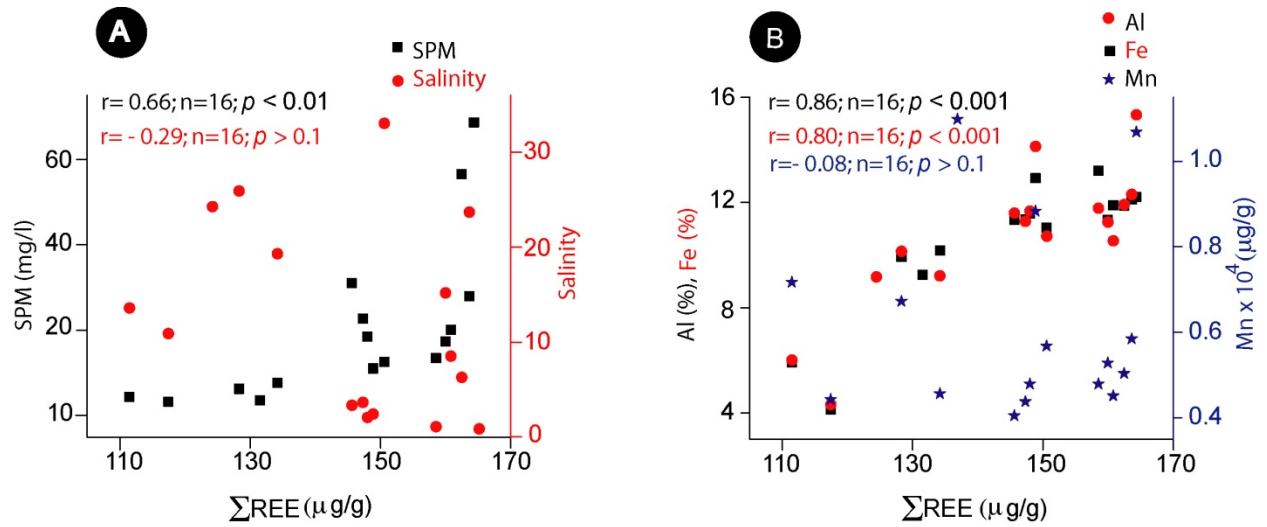
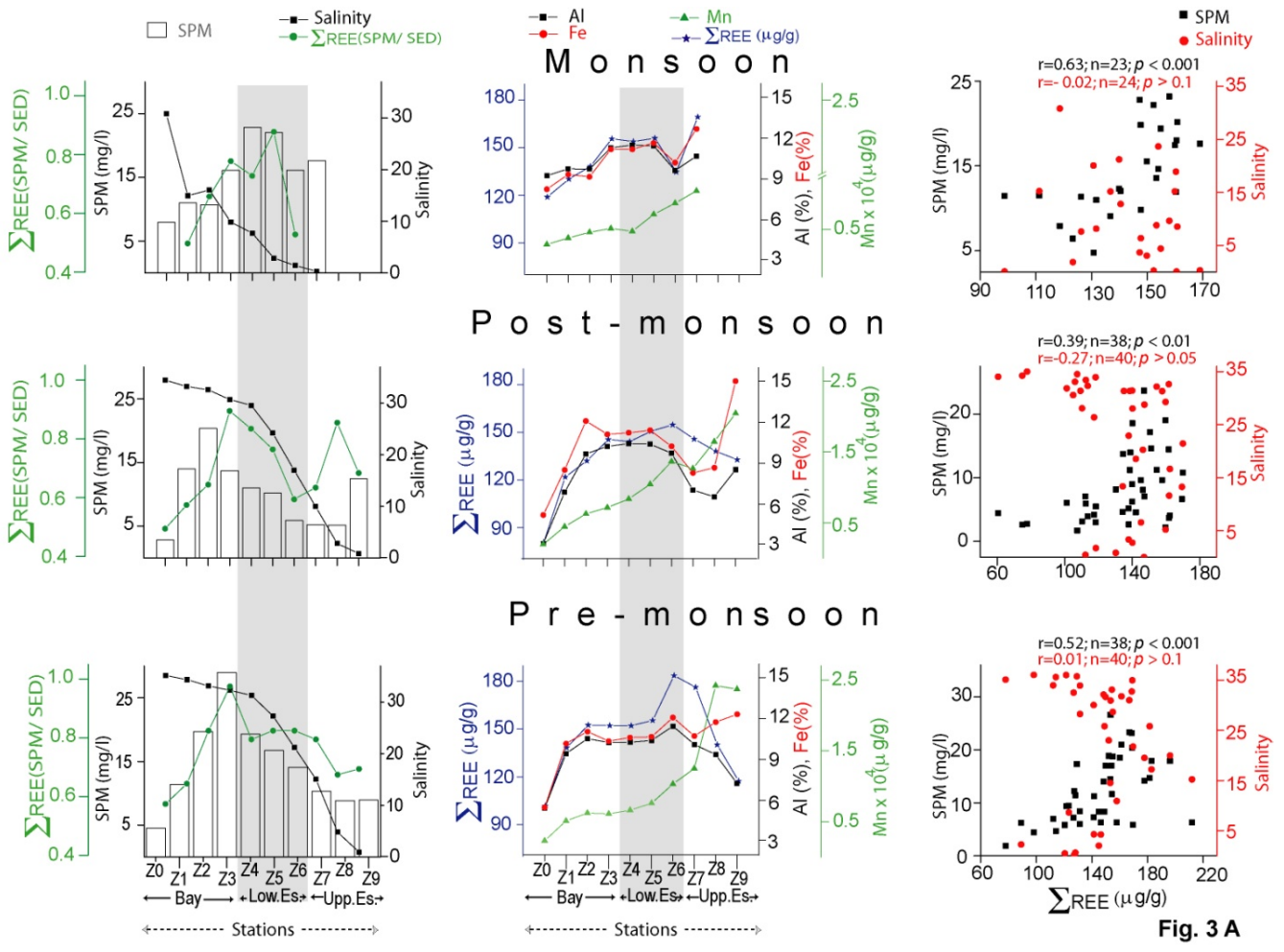


Fig. 2



**Fig. 3 A**

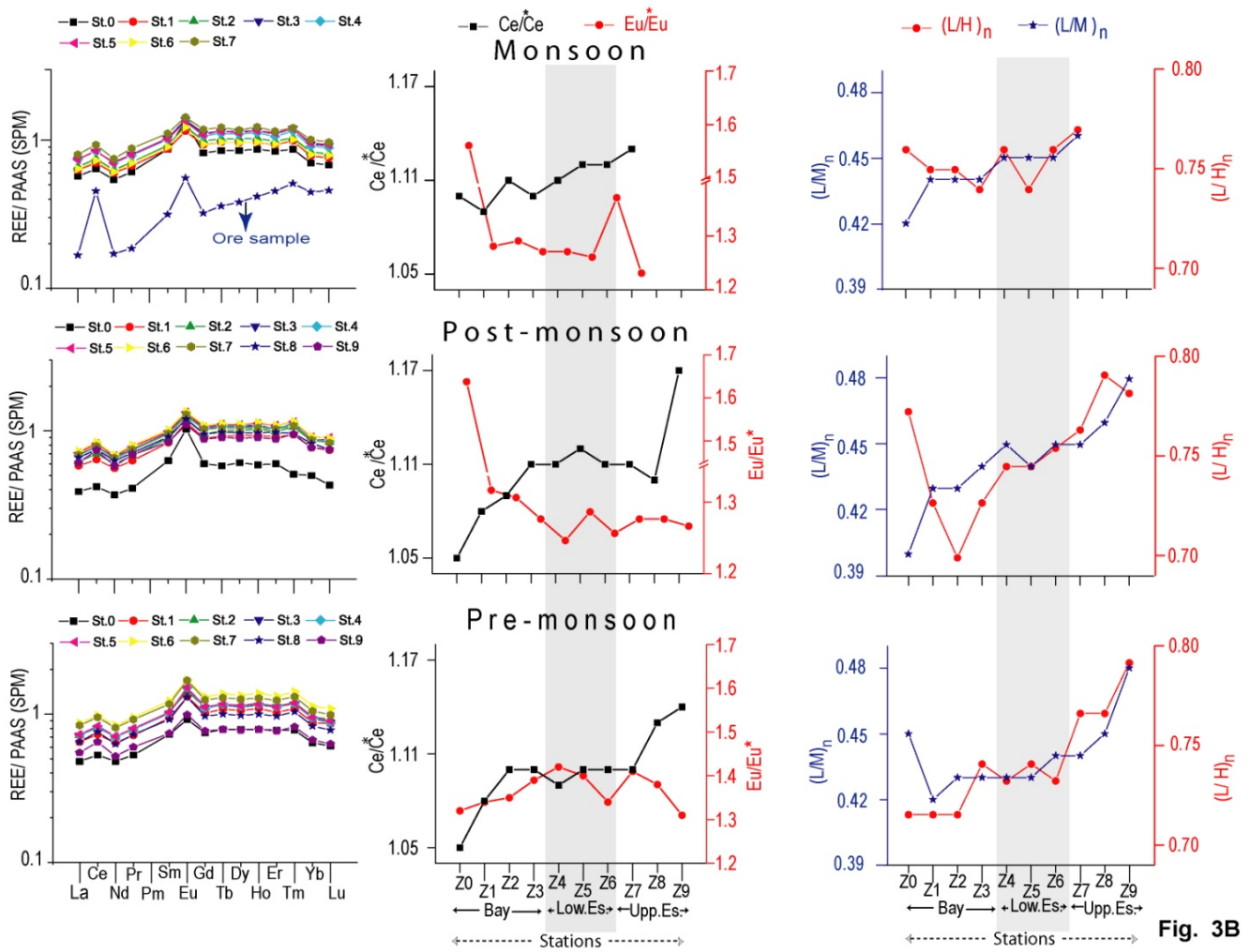


Fig. 3B

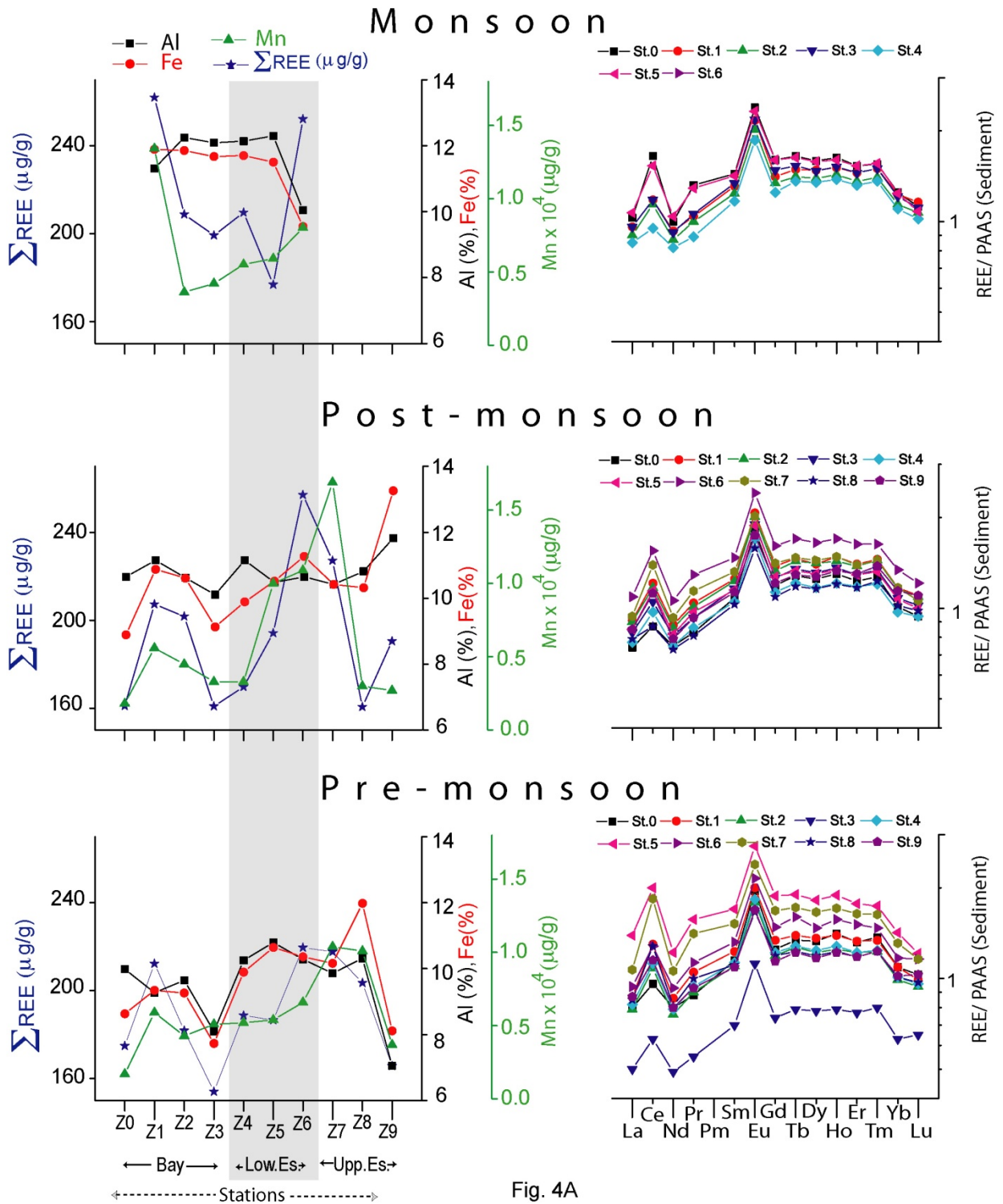


Fig. 4A



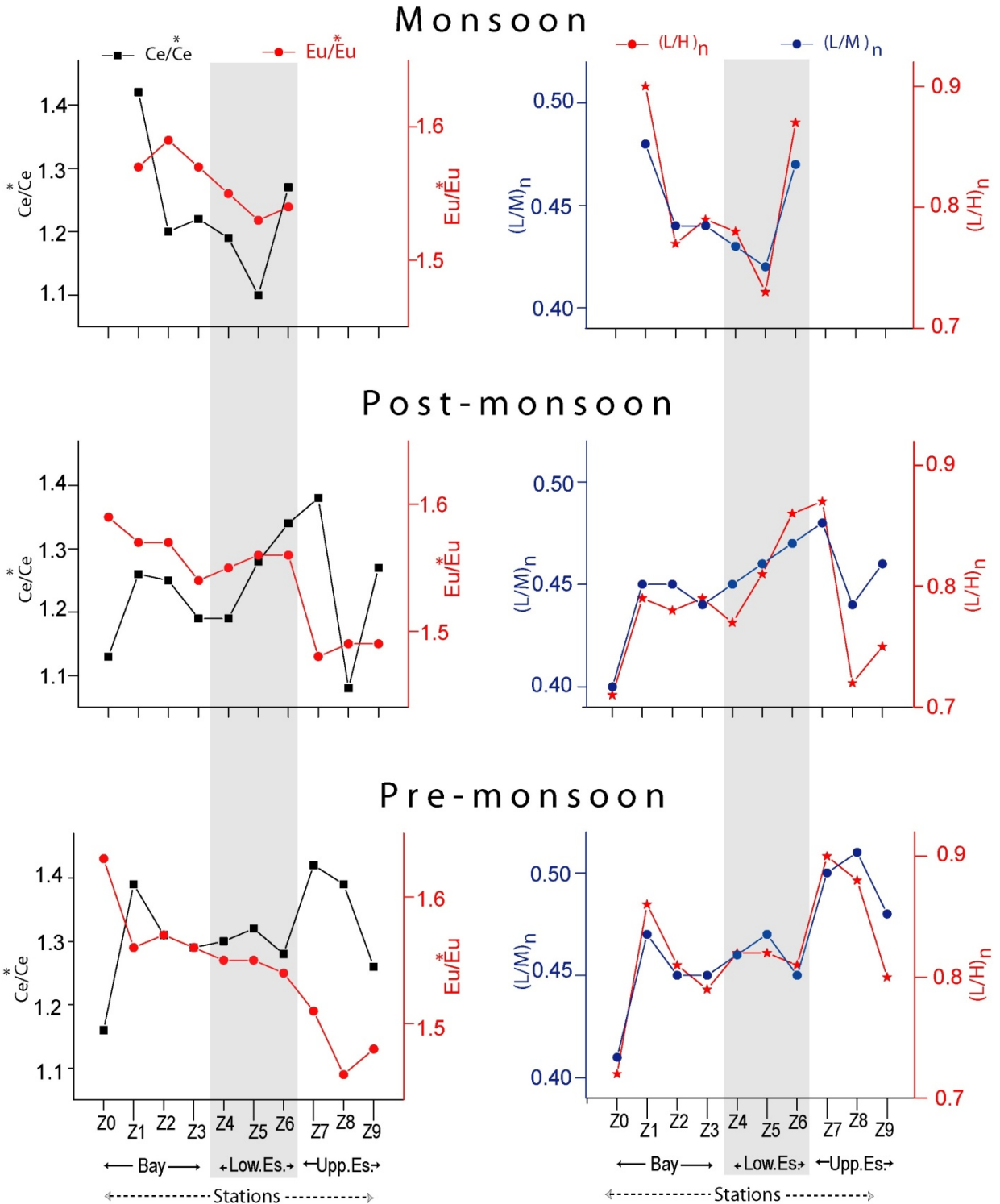


Fig. 4B

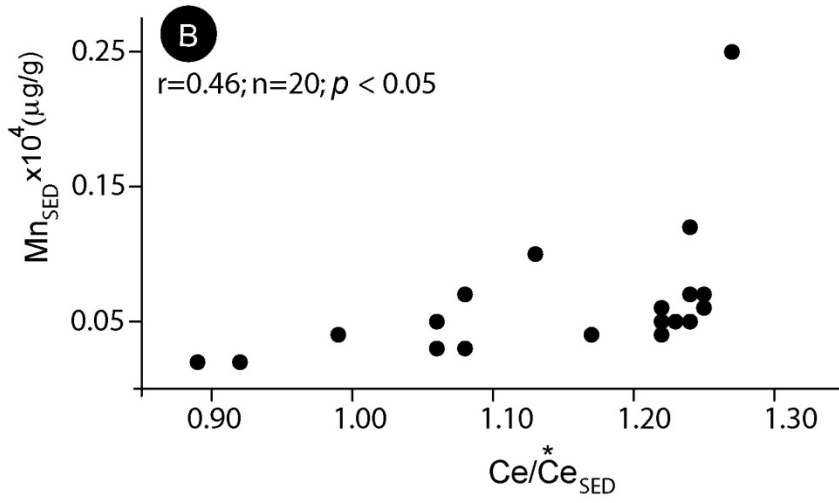
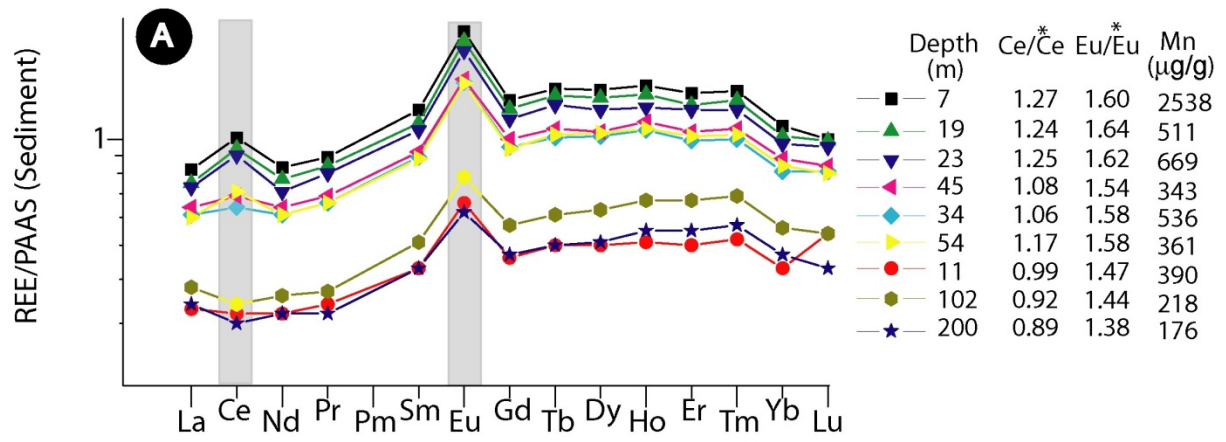


Fig.5

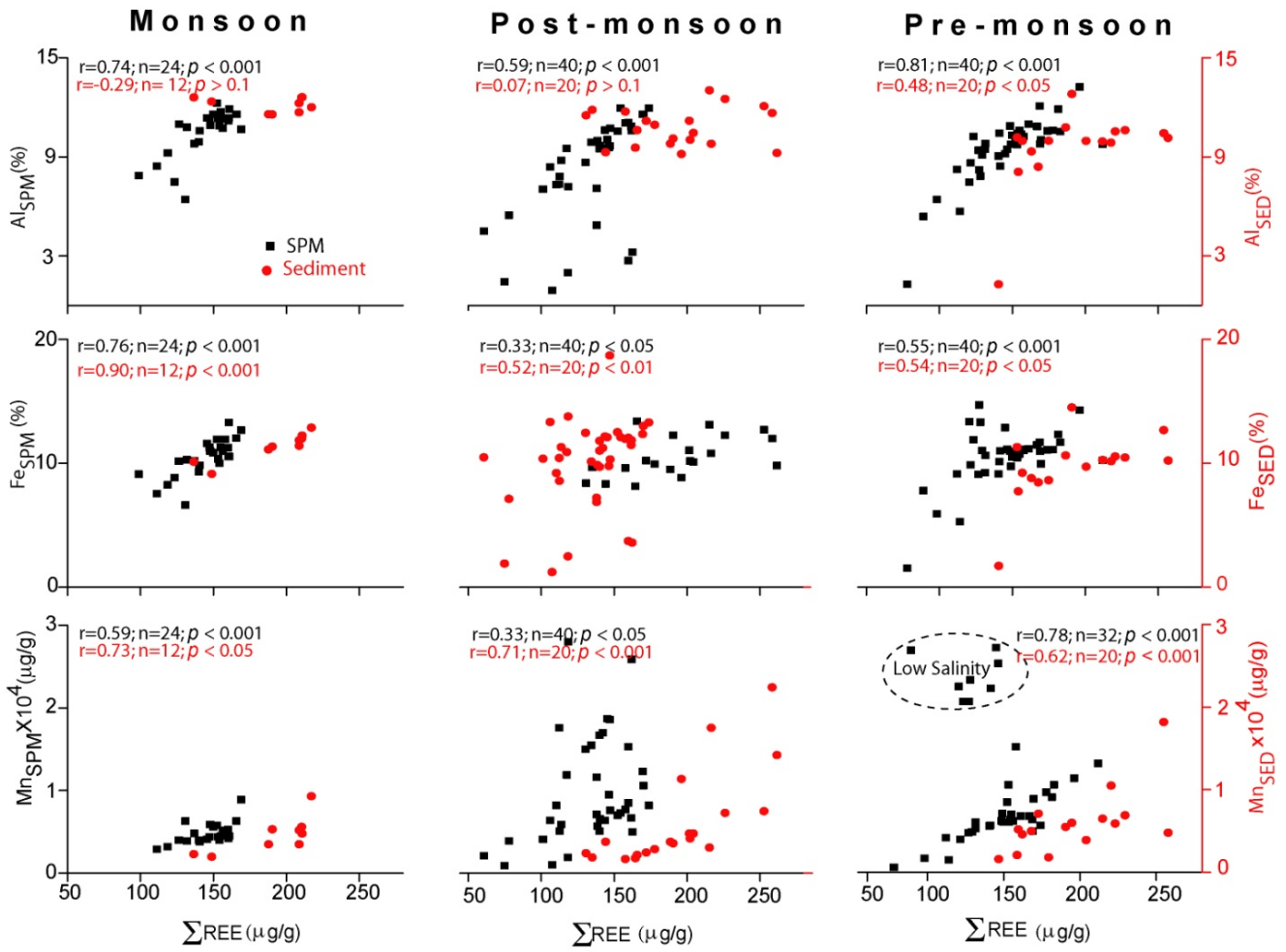
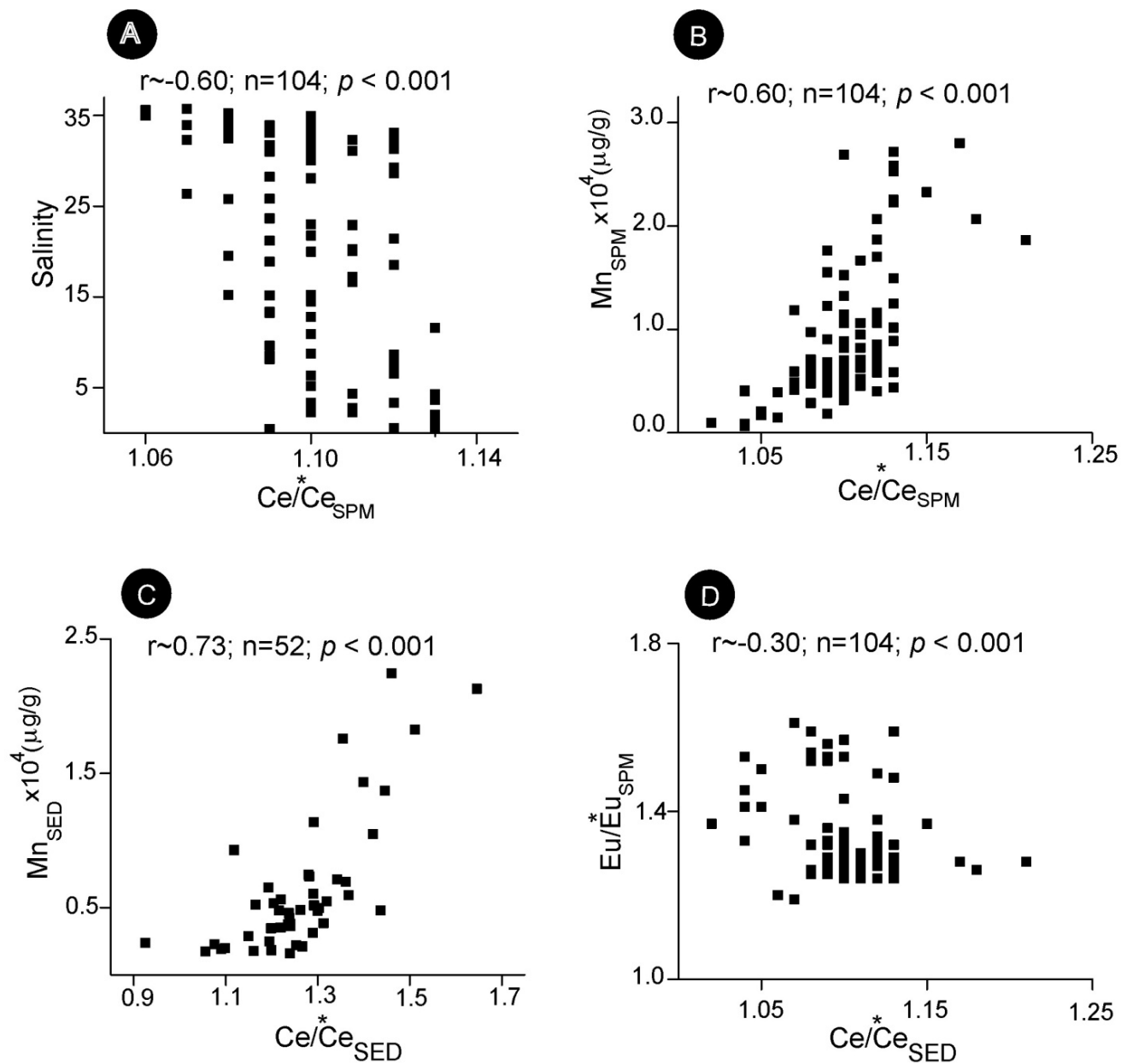


Fig. 6



**Fig. 7**

Table 1A  
 Number of samples analyzed at the regular and transect stations of the Zuari estuary during monsoon, post-monsoon and pre-monsoon.

Parameters	Regular Station	Transect Stations			Off-shore stations	Total number of samples analyzed	Instruments used	
	Monsoon	Monsoon	Post-monsoon	Pre-monsoon				
Suspended Particulate matter (SPM) {	Salinity	16	26	40	40	122	CTD	
	SPM concentration	16	26	40	40	122	Filtration unit	
	Major elements	16	26	40	40	122	ICP-AES	
	REE	16	26	40	40	122	ICP-MS	
Sediment {	Major elements		11	20	19	20	70	ICP-AES
	REE		11	20	19	20	70	ICP-MS

Table. 1B

Analytical results of certified and obtained values of USGS geochemical standard MAG-1 (all trace elements values are in  $\mu\text{g/g}$ )

Elements	USGS certified values.	This work	$\text{\$Accuracy (\%)}$	$\text{\$Precision (\%)}$
		Mean of 2 analysis	( $\pm$ )	( $\pm$ )
Al (%)	$8.66 \pm 0.16$	$8.81 \pm 0.11$	1.79	1.70
Fe (%)	$4.58 \pm 0.42$	$4.91 \pm 0.11$	7.21	3.25
Mn ( $\mu\text{g/g}$ )	$760 \pm 69$	$775.00 \pm 20$	3.13	3.35
La	$43 \pm 4$	$43.33 \pm 1.05$	0.77	3.41
Ce	$88 \pm 9$	$90.20 \pm 2.74$	2.50	4.30
Pr	9.3	$9.55 \pm 0.33$	2.68	4.82
Nd	$38 \pm 5$	$38.49 \pm 1.09$	1.29	4.00
Sm	$7.5 \pm 0.6$	$7.63 \pm 0.40$	1.75	7.41
Eu	$1.5 \pm 0.14$	$1.57 \pm 0.07$	1.87	6.33
Gd	$5.8 \pm 0.7$	$6.10 \pm 0.24$	5.18	5.45
Tb	$0.96 \pm 0.09$	$0.98 \pm 0.06$	3.02	8.89
Dy	$5.2 \pm 0.3$	$5.47 \pm 0.34$	5.20	8.68
Ho	$1.02 \pm 0.1$	$1.13 \pm 0.05$	10.78	5.84
Er	3	$3.10 \pm 0.13$	3.40	5.99
Tm	0.43	$0.47 \pm 0.02$	10.47	7.15
Yb	$2.6 \pm 0.3$	$2.66 \pm 0.06$	2.62	3.29
Lu	$0.4 \pm 0.04$	$0.40 \pm 0.02$	1.87	6.13

$$\text{\$Accuracy \%} = \left\{ \frac{\text{Mean} - \text{Certified value}}{\text{Certified value}} \right\} \times 100$$

$$\text{\$Precision \%} = \left\{ \frac{\text{Measured 1} - \text{Measured 2}}{\text{Average}} \right\} \times 100$$

Table 2

Concentrations of Al (%), Fe (%), Mn ( $\mu\text{g/g}$ ) and REEs ( $\mu\text{g/g}$ ) in suspended particulate matter (SPM-mg/l) at regular station in the Zuari estuary.

Dates	Salinity	SPM	Al	Fe	Mn	La	Ce	Pr	Nd	Sm	Eu	Gd	Tb	Dy	Ho	Er	Tm	Yb	Lu	$\Sigma\text{REE}$	$(\text{L}/\text{H})_n^a$	$(\text{L}/\text{M})_n^a$	$(\text{H}/\text{M})_n^a$	$\text{Ce}^*/\text{Ce}$	$\text{Eu}^*/\text{Eu}$
4 <sup>th</sup> Jun	33.0	12.7	11.0	10.7	5681	27.7	64.9	6.0	26.5	5.6	1.4	5.0	0.9	5.1	1.1	3.0	0.5	2.5	0.4	150.6	0.77	0.45	0.58	1.14	1.26
8 <sup>th</sup> Jun	23.7	28.0	12.1	12.3	5849	30.0	71.3	6.5	28.5	5.9	1.5	5.3	0.9	5.5	1.2	3.2	0.5	2.7	0.4	163.6	0.77	0.45	0.59	1.16	1.26
20 <sup>th</sup> Jun	8.5	20.2	11.9	10.5	4516	30.0	69.4	6.5	28.3	5.8	1.5	5.3	0.9	5.3	1.2	3.1	0.5	2.6	0.4	160.8	0.78	0.46	0.59	1.13	1.26
27 <sup>th</sup> Jun	2.1	18.6	11.6	11.7	4793	27.2	64.6	5.9	25.9	5.3	1.4	4.8	0.8	4.9	1.0	2.9	0.4	2.4	0.4	148.0	0.78	0.46	0.59	1.16	1.27
5 <sup>th</sup> Jul	6.3	56.5	11.9	11.9	5039	30.0	70.2	6.4	28.6	5.9	1.5	5.3	0.9	5.5	1.2	3.2	0.5	2.7	0.4	162.5	0.77	0.45	0.59	1.15	1.28
15 <sup>th</sup> Jul	19.3	7.7	10.2	9.2	4564	24.5	58.2	5.4	23.5	4.9	1.3	4.4	0.8	4.6	1.0	2.7	0.4	2.2	0.3	134.2	0.77	0.45	0.58	1.16	1.29
19 <sup>th</sup> Jul	15.2	17.4	11.3	11.3	5285	29.4	69.3	6.4	28.0	5.9	1.5	5.3	0.9	5.4	1.2	3.2	0.5	2.7	0.4	159.9	0.75	0.45	0.60	1.16	1.27
26 <sup>th</sup> Jul	1.1	13.5	13.2	11.8	4793	29.4	68.6	6.4	27.8	5.8	1.5	5.1	0.9	5.3	1.1	3.1	0.5	2.7	0.4	158.5	0.76	0.46	0.60	1.14	1.28
11 <sup>th</sup> Aug	0.0	68.6	12.2	15.3	10685	28.7	74.0	6.3	28.6	5.8	1.5	5.2	0.9	5.3	1.1	3.2	0.5	2.7	0.4	164.3	0.75	0.46	0.62	1.26	1.28
16 <sup>th</sup> Aug	3.4	31.0	11.3	11.6	4053	27.1	63.0	5.9	25.2	5.3	1.3	4.8	0.8	4.9	1.1	2.9	0.4	2.5	0.4	145.6	0.75	0.45	0.60	1.14	1.25
25 <sup>th</sup> Aug	13.6	4.4	5.9	6.0	7173	20.4	48.5	4.4	19.5	4.0	1.0	3.7	0.6	3.8	0.8	2.3	0.3	1.9	0.3	111.5	0.75	0.45	0.60	1.17	1.24
29 <sup>th</sup> Aug	25.9	6.3	9.9	10.1	6726	23.3	55.6	5.2	22.5	4.8	1.2	4.2	0.7	4.3	1.0	2.6	0.4	2.1	0.3	128.3	0.75	0.45	0.60	1.16	1.27
12 <sup>th</sup> Aug	2.4	11.1	12.9	14.1	8833	26.3	66.1	5.7	26.0	5.3	1.3	4.7	0.8	4.9	1.1	3.0	0.5	2.6	0.4	148.9	0.72	0.46	0.64	1.23	1.27
18 <sup>th</sup> Aug	3.7	22.7	11.3	11.3	4377	26.7	64.5	5.9	25.7	5.3	1.4	4.7	0.8	4.9	1.1	2.9	0.4	2.4	0.4	147.3	0.76	0.45	0.60	1.18	1.32
23 <sup>rd</sup> Aug	10.9	3.3	4.1	4.3	4428	22.2	50.5	4.7	20.8	4.2	1.0	3.9	0.6	3.9	0.8	2.3	0.3	1.9	0.3	117.4	0.81	0.47	0.58	1.12	1.19
16 <sup>th</sup> Oct	26.4	4.2	9.5	10.9	11857	23.9	57.3	5.3	23.0	4.8	1.2	4.4	0.7	4.5	0.9	2.7	0.4	2.2	0.3	131.7	0.75	0.45	0.60	1.17	1.27
Mean	<b>12.2</b>	<b>20.4</b>	<b>10.7</b>	<b>10.8</b>	<b>6166</b>	<b>26.7</b>	<b>63.5</b>	<b>5.8</b>	<b>25.5</b>	<b>5.3</b>	<b>1.4</b>	<b>4.8</b>	<b>0.8</b>	<b>4.9</b>	<b>1.1</b>	<b>2.9</b>	<b>0.4</b>	<b>2.4</b>	<b>0.4</b>	<b>145.8</b>	<b>0.76</b>	<b>0.46</b>	<b>0.60</b>	<b>1.16</b>	<b>1.27</b>
	$\pm 10.6$	$\pm 18.6$	$\pm 2.4$	$\pm 2.7$	$\pm 2358$	$\pm 3.0$	$\pm 7.5$	$\pm 0.7$	$\pm 2.9$	$\pm 0.6$	$\pm 0.2$	$\pm 0.5$	$\pm 0.1$	$\pm 0.5$	$\pm 0.1$	$\pm 0.3$	$\pm 0.1$	$\pm 0.3$	$\pm 0.0$	$\pm 16.7$	$\pm 0.02$	$\pm 0.01$	$\pm 0.01$	$\pm 0.03$	$\pm 0.03$
PAAS <sup>b</sup>			10.0	4.5	800	38.2	79.6	8.8	33.9	5.6	1.1	4.7	0.8	4.7	1.0	2.9	0.4	2.8	0.4	184.8					
ASSWR <sup>c</sup>			8.7	5.8	1679	37.4	73.6	8.0	32.2	6.1	1.3	5.3	0.8	4.3	0.9	2.2	0.4	2.1	0.4	174.8	1.15	0.60	0.52	0.97	1.07
UCC <sup>d</sup>			8.0	3.5	600	30.0	64.0	7.1	26.0	4.5	0.9	3.8	0.6	3.5	0.8	2.3	0.3	2.2	0.3	146.4	1.01	0.66	0.65	1.02	1.00

$\text{Ce}/\text{Ce}^*$  (Ce anomaly) =  $3\text{Ce}_{\text{CN}}/(2\text{La}_{\text{CN}} + \text{Nd}_{\text{CN}})$  and  $\text{Eu}/\text{Eu}^*$  (Eu anomaly) =  $\text{Eu}_{\text{CN}}/(\text{Sm}_{\text{CN}} \times \text{Gd}_{\text{CN}})^{1/2}$  (Taylor and McLennan, 1985)

<sup>a</sup>  $(\text{L}/\text{H})_n$ ,  $(\text{L}/\text{M})_n$  and  $(\text{H}/\text{M})_n$  are PAAS normalized LREE/HREE, LREE/MREE and HREE/MREE. LREE are La to Nd, MREE are Sm to Ho and HREE are Er to Lu (Rollinson, 1993).

<sup>b</sup> PAAS - Post-Archaean average Australian shale (McLennan, 1989)

<sup>c</sup> ASSWR - Average suspended sediment in World Rivers (Viers et al., 2009)

<sup>d</sup> UCC - Upper continental crust (Taylor and McLennan, 1985)

Table 3

Concentrations of Al (%), Fe (%), Mn ( $\mu\text{g/g}$ ) and REEs ( $\mu\text{g/g}$ ) in suspended particulate matter (SPM-mg/l) at transect stations in the Zuari estuary.

Stns.	Salinity	SPM	Al	Fe	Mn	La	Ce	Pr	Nd	Sm	Eu	Gd	Tb	Dy	Ho	Er	Tm	Yb	Lu	$\Sigma\text{REE}$	(L/H) <sub>n</sub>	(L/M) <sub>n</sub>	(H/M) <sub>n</sub>	Ce/Ce*	Eu/Eu*	
<b>M o n s o o n (June to September)</b>																										
Z 0 (1)	30.8	7.9	9.2	8.2	3162	21.7	51.0	4.7	20.6	4.9	1.4	3.8	0.7	4.0	0.9	2.4	0.4	2.0	0.3	118.6	0.76	0.42	0.55	1.10	1.57	
Z 1 (4)	14.9	11.0	9.7	9.3	3908	24.0	55.6	5.3	22.8	4.8	1.2	4.3	0.8	4.5	1.0	2.6	0.4	2.2	0.3	129.9	0.75	0.44	0.59	1.09	1.28	
	$\pm 5.3$	$\pm 1.4$	$\pm 1.0$	$\pm 1.3$	$\pm 798$	$\pm 2.3$	$\pm 5.6$	$\pm 0.5$	$\pm 2.3$	$\pm 0.5$	$\pm 0.1$	$\pm 0.4$	$\pm 0.1$	$\pm 0.4$	$\pm 0.1$	$\pm 0.3$	$\pm 0.0$	$\pm 0.2$	$\pm 0.0$	$\pm 12.9$	$\pm 0.01$	$\pm 0.01$	$\pm 0.01$	$\pm 0.00$	$\pm 0.05$	
Z 2 (4)	16.0	10.7	9.7	9.2	4535	25.1	59.5	5.5	24.1	5.1	1.3	4.6	0.8	4.8	1.0	2.8	0.4	2.3	0.4	137.8	0.75	0.44	0.59	1.11	1.30	
	$\pm 7.2$	$\pm 4.2$	$\pm 2.2$	$\pm 1.7$	$\pm 1179$	$\pm 2.4$	$\pm 4.9$	$\pm 0.6$	$\pm 2.1$	$\pm 0.4$	$\pm 0.1$	$\pm 0.5$	$\pm 0.1$	$\pm 0.5$	$\pm 0.1$	$\pm 0.3$	$\pm 0.1$	$\pm 0.2$	$\pm 0.0$	$\pm 12.3$	$\pm 0.01$	$\pm 0.01$	$\pm 0.01$	$\pm 0.01$	$\pm 0.06$	
Z 3 (4)	9.8	16.1	11.3	11.2	4904	28.4	66.8	6.3	27.3	5.7	1.5	5.2	0.9	5.3	1.1	3.1	0.5	2.7	0.4	155.2	0.74	0.44	0.60	1.10	1.28	
	$\pm 6.4$	$\pm 6.3$	$\pm 0.3$	$\pm 0.6$	$\pm 731$	$\pm 1.1$	$\pm 2.3$	$\pm 0.2$	$\pm 1.0$	$\pm 0.2$	$\pm 0.1$	$\pm 0.2$	$\pm 0.0$	$\pm 0.2$	$\pm 0.0$	$\pm 0.1$	$\pm 0.0$	$\pm 0.1$	$\pm 0.0$	$\pm 5.5$	$\pm 0.01$	$\pm 0.00$	$\pm 0.01$	$\pm 0.01$	$\pm 0.02$	
Z 4 (4)	7.7	22.9	11.5	11.2	4558	28.3	66.5	6.2	26.8	5.6	1.4	5.0	0.9	5.1	1.1	3.0	0.5	2.6	0.4	153.4	0.76	0.45	0.60	1.10	1.28	
	$\pm 5.5$	$\pm 5.9$	$\pm 0.3$	$\pm 0.4$	$\pm 522$	$\pm 1.6$	$\pm 3.3$	$\pm 0.3$	$\pm 1.6$	$\pm 0.3$	$\pm 0.1$	$\pm 0.3$	$\pm 0.0$	$\pm 0.3$	$\pm 0.1$	$\pm 0.1$	$\pm 0.0$	$\pm 0.1$	$\pm 0.0$	$\pm 8.1$	$\pm 0.01$	$\pm 0.00$	$\pm 0.01$	$\pm 0.02$	$\pm 0.03$	
Z 5 (4)	2.9	22.0	11.4	11.6	6393	28.3	67.6	6.2	27.2	5.7	1.4	5.1	0.9	5.2	1.1	3.2	0.5	2.7	0.4	155.6	0.74	0.45	0.61	1.11	1.26	
	$\pm 4.1$	$\pm 8.9$	$\pm 0.6$	$\pm 1.3$	$\pm 2587$	$\pm 0.5$	$\pm 1.8$	$\pm 0.1$	$\pm 0.6$	$\pm 0.2$	$\pm 0.0$	$\pm 0.1$	$\pm 0.0$	$\pm 0.1$	$\pm 0.0$	$\pm 0.1$	$\pm 0.0$	$\pm 0.1$	$\pm 0.0$	$\pm 3.7$	$\pm 0.02$	$\pm 0.00$	$\pm 0.01$	$\pm 0.02$	$\pm 0.01$	
Z 6 (4)	1.4	16.1	9.6	10.2	7555	24.4	58.5	5.4	23.6	5.0	1.3	4.4	0.7	4.5	1.0	2.7	0.4	2.2	0.3	134.4	0.76	0.45	0.59	1.12	1.35	
	$\pm 1.3$	$\pm 10.6$	$\pm 2.3$	$\pm 1.5$	$\pm 3305$	$\pm 5.5$	$\pm 12.7$	$\pm 1.2$	$\pm 5.3$	$\pm 1.0$	$\pm 0.2$	$\pm 1.1$	$\pm 0.2$	$\pm 1.1$	$\pm 0.2$	$\pm 0.6$	$\pm 0.1$	$\pm 0.5$	$\pm 0.1$	$\pm 29.6$	$\pm 0.02$	$\pm 0.02$	$\pm 0.02$	$\pm 0.01$	$\pm 0.16$	
Z 7 (1)	0.3	17.6	10.7	12.7	8891	30.5	74.2	6.7	29.7	6.2	1.5	5.5	0.9	5.5	1.2	3.3	0.5	2.8	0.4	168.9	0.77	0.46	0.59	1.13	1.24	
<b>P o s t - m o n s o o n (October to January)</b>																										
Z 0 (4)	34.5	2.9	3.1	5.2	1961	14.9	33.1	3.3	14.0	3.5	1.1	2.8	0.4	2.9	0.6	1.7	0.2	1.4	0.2	80.1	0.77	0.40	0.51	1.05	1.68	
	$\pm 0.4$	$\pm 1.1$	$\pm 2.2$	$\pm 4.4$	$\pm 1426$	$\pm 4.0$	$\pm 8.1$	$\pm 0.8$	$\pm 3.5$	$\pm 0.9$	$\pm 0.4$	$\pm 0.7$	$\pm 0.1$	$\pm 0.7$	$\pm 0.1$	$\pm 0.4$	$\pm 0.0$	$\pm 0.3$	$\pm 0.0$	$\pm 19.7$	$\pm 0.08$	$\pm 0.05$	$\pm 0.05$	$\pm 0.02$	$\pm 0.49$	
Z 1 (4)	33.2	14.0	6.9	8.5	4519	22.1	51.2	5.0	21.3	4.6	1.2	4.1	0.7	4.4	0.9	2.6	0.4	2.2	0.3	121.0	0.72	0.43	0.60	1.08	1.33	
	$\pm 1.0$	$\pm 18.1$	$\pm 3.6$	$\pm 4.3$	$\pm 2141$	$\pm 3.7$	$\pm 9.7$	$\pm 0.9$	$\pm 3.9$	$\pm 0.8$	$\pm 0.2$	$\pm 0.8$	$\pm 0.1$	$\pm 0.8$	$\pm 0.2$	$\pm 0.5$	$\pm 0.1$	$\pm 0.4$	$\pm 0.1$	$\pm 22.0$	$\pm 0.05$	$\pm 0.01$	$\pm 0.03$	$\pm 0.03$	$\pm 0.06$	
Z 2 (4)	32.6	20.3	9.7	12.1	6346	23.8	56.0	5.3	23.0	5.0	1.3	4.4	0.8	4.7	1.0	2.8	0.4	2.4	0.4	131.2	0.69	0.43	0.62	1.09	1.32	
	$\pm 0.4$	$\pm 21.1$	$\pm 1.2$	$\pm 0.9$	$\pm 319$	$\pm 4.7$	$\pm 11.6$	$\pm 1.1$	$\pm 4.6$	$\pm 0.9$	$\pm 0.2$	$\pm 0.8$	$\pm 0.1$	$\pm 0.9$	$\pm 0.2$	$\pm 0.5$	$\pm 0.1$	$\pm 0.4$	$\pm 0.1$	$\pm 25.9$	$\pm 0.04$	$\pm 0.01$	$\pm 0.03$	$\pm 0.02$	$\pm 0.05$	
Z 3 (4)	30.7	13.7	10.2	11.1	7217	26.2	62.3	5.9	25.4	5.4	1.4	4.8	0.8	5.0	1.1	2.9	0.5	2.5	0.4	144.6	0.75	0.44	0.60	1.11	1.29	
	$\pm 1.8$	$\pm 12.3$	$\pm 2.2$	$\pm 1.9$	$\pm 1449$	$\pm 4.5$	$\pm 11.3$	$\pm 1.0$	$\pm 4.6$	$\pm 1.0$	$\pm 0.3$	$\pm 1.0$	$\pm 0.2$	$\pm 1.2$	$\pm 0.2$	$\pm 0.6$	$\pm 0.1$	$\pm 0.5$	$\pm 0.1$	$\pm 26.7$	$\pm 0.05$	$\pm 0.02$	$\pm 0.01$	$\pm 0.01$	$\pm 0.03$	
Z 4 (4)	29.6	11.0	10.4	11.2	8448	26.0	61.9	5.7	25.2	5.3	1.4	4.8	0.8	4.9	1.1	3.0	0.4	2.5	0.4	143.4	0.74	0.45	0.60	1.11	1.26	
	$\pm 2.4$	$\pm 6.1$	$\pm 0.8$	$\pm 1.0$	$\pm 2561$	$\pm 2.9$	$\pm 8.7$	$\pm 0.8$	$\pm 3.4$	$\pm 0.8$	$\pm 0.2$	$\pm 0.7$	$\pm 0.1$	$\pm 0.8$	$\pm 0.2$	$\pm 0.5$	$\pm 0.1$	$\pm 0.4$	$\pm 0.1$	$\pm 19.7$	$\pm 0.04$	$\pm 0.02$	$\pm 0.01$	$\pm 0.03$	$\pm 0.05$	
Z 5 (4)	24.2	10.2	10.4	11.4	10457	27.0	65.0	6.0	26.3	5.5	1.5	5.0	0.9	5.2	1.1	3.1	0.5	2.6	0.4	149.8	0.74	0.44	0.60	1.12	1.30	
	$\pm 5.0$	$\pm 6.1$	$\pm 1.0$	$\pm 1.1$	$\pm 4706$	$\pm 2.3$	$\pm 6.1$	$\pm 0.6$	$\pm 2.5$	$\pm 0.6$	$\pm 0.2$	$\pm 0.5$	$\pm 0.1$	$\pm 0.5$	$\pm 0.1$	$\pm 0.3$	$\pm 0.0$	$\pm 0.2$	$\pm 0.0$	$\pm 13.7$	$\pm 0.02$	$\pm 0.01$	$\pm 0.01$	$\pm 0.01$	$\pm 0.03$	



Table. 3 (Continued)

Stns.	Salinity	SPM	Al	Fe	Mn	La	Ce	Pr	Nd	Sm	Eu	Gd	Tb	Dy	Ho	Er	Tm	Yb	Lu	$\sum$ REE (L/H) <sub>n</sub>	(L/M) <sub>n</sub>	(H/M) <sub>n</sub>	Ce/Ĉe	Eu/Ēu	
<b>P o s t - m o n s o o n (continued)</b>																									
Z 6 (4)	17.0 ±5.4	5.9 ±1.9	9.7 ±1.9	10.2 ±2.5	13678 ±8391	28.0 ±2.6	66.7 ±6.2	6.1 ±0.6	27.0 ±2.6	5.7 ±0.6	1.5 ±0.2	5.1 ±0.5	0.9 ±0.1	5.2 ±0.5	1.1 ±0.1	3.1 ±0.3	0.5 ±0.0	2.6 ±0.2	0.4 ±0.0	153.9 ±14.4	0.75 ±0.02	0.45 ±0.01	0.60 ±0.01	1.11 ±0.02	1.27 ±0.04
Z 7 (4)	10.0 ±6.1	5.2 ±3.0	7.0 ±3.5	8.3 ±3.7	12708 ±5918	26.5 ±2.4	62.9 ±5.7	5.8 ±0.5	25.4 ±2.1	5.3 ±0.5	1.4 ±0.1	4.8 ±0.4	0.8 ±0.1	4.9 ±0.4	1.0 ±0.1	2.9 ±0.2	0.4 ±0.0	2.5 ±0.2	0.4 ±0.0	145.0 ±12.4	0.76 ±0.03	0.45 ±0.01	0.59 ±0.01	1.11 ±0.01	1.29 ±0.02
Z 8 (4)	2.8 ±2.4	5.2 ±2.6	6.5 ±3.5	8.6 ±4.3	16522 ±1171	25.3 ±4.3	59.5 ±10.1	5.5 ±0.9	24.2 ±4.0	5.1 ±1.0	1.3 ±0.2	4.4 ±0.9	0.8 ±0.1	4.5 ±0.9	1.0 ±0.2	2.8 ±0.6	0.4 ±0.1	2.3 ±0.5	0.3 ±0.0	137.3 ±23.8	0.79 ±0.02	0.46 ±0.01	0.59 ±0.01	1.10 ±0.01	1.29 ±0.02
Z 9 (4)	0.9 ±0.8	12.4 ±9.8	8.5 ±1.2	15.0 ±3.3	20539 ±6751	23.2 ±2.2	59.1 ±7.1	5.2 ±0.5	23.3 ±2.5	4.6 ±0.4	1.2 ±0.1	4.1 ±0.4	0.7 ±0.1	4.2 ±0.4	0.9 ±0.1	2.5 ±0.3	0.4 ±0.0	2.2 ±0.2	0.3 ±0.0	131.9 ±14.3	0.78 ±0.03	0.48 ±0.01	0.61 ±0.01	1.17 ±0.04	1.28 ±0.01
<b>P r e - m o n s o o n</b>																									
Z 0 (4)	35.2 ±0.9	4.5 ±2.1	5.4 ±3.0	5.5 ±3.1	1984 ±1515	18.4 ±3.2	41.9 ±7.6	4.2 ±0.7	18.0 ±3.0	4.1 ±0.7	0.7 ±0.5	3.5 ±0.6	0.6 ±0.1	3.7 ±0.4	0.8 ±0.1	2.2 ±0.3	0.3 ±0.0	1.8 ±0.2	0.3 ±0.0	100.6 ±16.7	0.71 ±0.04	0.45 ±0.06	0.62 ±0.07	1.05 ±0.01	1.32 ±0.09
Z 1 (4)	34.3 ±1.5	11.4 ±6.1	9.4 ±0.6	10.1 ±0.8	4777 ±557	24.9 ±3.6	57.8 ±9.6	5.7 ±0.9	24.4 ±3.8	5.2 ±0.8	1.4 ±0.2	4.7 ±0.7	0.8 ±0.1	5.0 ±0.8	1.1 ±0.2	2.9 ±0.5	0.4 ±0.1	2.5 ±0.4	0.4 ±0.1	137.2 ±21.6	0.71 ±0.02	0.42 ±0.01	0.59 ±0.02	1.08 ±0.03	1.34 ±0.13
Z 2 (4)	33.1 ±2.0	19.7 ±6.6	10.5 ±1.2	11.0 ±0.5	5941 ±718	27.3 ±2.8	64.6 ±7.6	6.2 ±0.6	26.7 ±2.9	5.7 ±0.7	1.5 ±0.1	5.2 ±0.5	0.9 ±0.1	5.4 ±0.5	1.2 ±0.1	3.2 ±0.3	0.5 ±0.0	2.7 ±0.2	0.4 ±0.0	151.4 ±16.4	0.71 ±0.01	0.43 ±0.01	0.60 ±0.01	1.10 ±0.02	1.35 ±0.18
Z 3 (4)	32.3 ±2.2	28.9 ±22.3	10.2 ±0.8	10.3 ±0.9	5811 ±303	27.4 ±2.9	64.5 ±6.2	6.1 ±0.7	26.7 ±3.0	5.6 ±0.5	1.6 ±0.3	5.2 ±0.6	0.9 ±0.1	5.2 ±0.6	1.1 ±0.1	3.2 ±0.4	0.5 ±0.1	2.6 ±0.3	0.4 ±0.0	151.1 ±15.7	0.74 ±0.03	0.43 ±0.01	0.58 ±0.02	1.10 ±0.01	1.39 ±0.12
Z 4 (4)	31.3 ±2.4	19.3 ±0.5	10.2 ±0.6	10.6 ±1.0	6298 ±318	27.4 ±2.7	64.4 ±6.3	6.2 ±0.6	26.7 ±2.8	5.6 ±0.5	1.6 ±0.3	5.1 ±0.5	0.9 ±0.1	5.3 ±0.5	1.2 ±0.1	3.2 ±0.3	0.5 ±0.0	2.6 ±0.2	0.4 ±0.0	151.0 ±14.9	0.73 ±0.03	0.43 ±0.01	0.58 ±0.03	1.09 ±0.01	1.42 ±0.16
Z 5 (4)	27.3 ±3.7	16.7 ±5.7	10.4 ±0.5	10.6 ±0.6	7348 ±748	28.0 ±0.9	66.1 ±2.1	6.3 ±0.3	27.3 ±0.8	5.7 ±0.3	1.6 ±0.2	5.2 ±0.2	0.9 ±0.0	5.3 ±0.2	1.2 ±0.1	3.2 ±0.1	0.5 ±0.0	2.7 ±0.1	0.4 ±0.0	154.4 ±5.2	0.74 ±0.03	0.43 ±0.01	0.58 ±0.03	1.10 ±0.01	1.40 ±0.17
Z 6 (4)	21.2 ±3.6	14.1 ±5.7	11.4 ±1.4	12.1 ±1.8	9989 ±1249	33.2 ±2.1	78.3 ±4.8	7.4 ±0.5	32.1 ±2.0	6.8 ±0.3	1.8 ±0.2	6.1 ±0.3	1.1 ±0.1	6.3 ±0.3	1.4 ±0.1	3.8 ±0.2	0.6 ±0.0	3.2 ±0.2	0.5 ±0.0	182.5 ±10.9	0.73 ±0.01	0.44 ±0.01	0.59 ±0.02	1.10 ±0.01	1.34 ±0.12
Z 7 (4)	15.1 ±3.5	10.3 ±4.6	10.1 ±0.4	10.7 ±0.4	12206 ±2508	31.9 ±4.9	75.3 ±11.5	7.1 ±1.1	31.2 ±4.8	6.5 ±1.1	1.8 ±0.3	5.8 ±0.9	1.0 ±0.2	5.9 ±0.9	1.3 ±0.2	3.5 ±0.5	0.5 ±0.1	2.9 ±0.4	0.4 ±0.1	175.2 ±26.7	0.77 ±0.02	0.44 ±0.01	0.58 ±0.02	1.10 ±0.01	1.41 ±0.14
Z 8 (4)	4.8 ±2.8	8.9 ±2.1	9.3 ±0.7	11.7 ±0.9	23870 ±2930	24.9 ±1.9	60.8 ±4.8	5.6 ±0.4	24.6 ±1.8	5.1 ±0.4	1.4 ±0.1	4.5 ±0.4	0.8 ±0.1	4.6 ±0.3	1.0 ±0.1	2.8 ±0.2	0.4 ±0.0	2.3 ±0.3	0.3 ±0.0	139.1 ±10.7	0.77 ±0.03	0.45 ±0.01	0.59 ±0.03	1.13 ±0.01	1.38 ±0.12
Z 9 (4)	0.9 ±0.9	8.9 ±3.4	7.2 ±1.3	12.3 ±3.1	23350 ±2618	21.0 ±3.1	51.7 ±8.8	4.6 ±0.7	20.5 ±3.1	4.1 ±0.6	1.1 ±0.2	3.6 ±0.5	0.6 ±0.1	3.6 ±0.5	0.8 ±0.1	2.2 ±0.3	0.3 ±0.0	1.9 ±0.3	0.3 ±0.1	116.2 ±18.4	0.80 ±0.03	0.48 ±0.01	0.59 ±0.02	1.14 ±0.03	1.31 ±0.05

The number in brackets in the first column indicates the number of samples analyzed at each station.

Table 4  
Concentrations of Al (%), Fe (%), Mn ( $\mu\text{g/g}$ ) and REEs ( $\mu\text{g/g}$ ) in surface sediments at transect stations in the Zuari estuary.

Stns	Al	Fe	Mn	La	Ce	Pr	Nd	Sm	Eu	Gd	Tb	Dy	Ho	Er	Tm	Yb	Lu	$\Sigma\text{REE (L/H)}_n$	$(\text{L/M})_n$	$(\text{H/M})_n$	$\text{Ce}^*/\text{Ce}$	$\text{Eu}^*/\text{Eu}$	
<b>M o n s o o n (August and September)</b>																							
Z 1 (2)	11.3 $\pm 0.4$	11.9 $\pm 0.8$	13322 $\pm 11281$	39.3 $\pm 8.8$	131.7 $\pm 64.6$	8.8 $\pm 2.0$	44.7 $\pm 17.2$	8.0 $\pm 2.0$	2.6 $\pm 0.7$	7.5 $\pm 1.9$	1.3 $\pm 0.3$	7.4 $\pm 1.8$	1.6 $\pm 0.4$	4.4 $\pm 0.9$	0.6 $\pm 0.1$	3.5 $\pm 0.7$	0.5 $\pm 0.1$	262.0 $\pm 101.5$	0.90 $\pm 0.15$	0.48 $\pm 0.05$	0.53 $\pm 0.03$	1.42 $\pm 0.31$	1.57 $\pm 0.02$
Z 2 (1)	12.3	11.8	3460	36.7	94.1	8.3	35.2	7.3	2.3	6.6	1.2	6.9	1.5	4.1	0.6	3.5	0.5	208.7	0.77	0.44	0.57	1.20	1.59
Z 3 (2)	12.1 $\pm 0.7$	11.7 $\pm 0.8$	4146 $\pm 908$	34.4 $\pm 2.4$	90.6 $\pm 7.0$	7.7 $\pm 0.7$	34.0 $\pm 3.2$	6.9 $\pm 0.6$	2.2 $\pm 0.2$	6.2 $\pm 0.5$	1.1 $\pm 0.1$	6.5 $\pm 0.7$	1.4 $\pm 0.1$	3.9 $\pm 0.3$	0.6 $\pm 0.1$	3.2 $\pm 0.3$	0.5 $\pm 0.0$	199.2 $\pm 16.2$	0.79 $\pm 0.00$	0.44 $\pm 0.01$	0.56 $\pm 0.00$	1.22 $\pm 0.00$	1.57 $\pm 0.03$
Z 4 (2)	12.1 $\pm 0.6$	11.7 $\pm 0.4$	5413 $\pm 283$	36.7 $\pm 0.5$	94.1 $\pm 2.3$	8.1 $\pm 0.2$	35.9 $\pm 0.1$	7.4 $\pm 0.1$	2.4 $\pm 0.1$	6.9 $\pm 0.1$	1.2 $\pm 0.0$	6.9 $\pm 0.1$	1.5 $\pm 0.0$	4.1 $\pm 0.1$	0.6 $\pm 0.0$	3.4 $\pm 0.0$	0.5 $\pm 0.0$	209.6 $\pm 1.2$	0.78 $\pm 0.01$	0.43 $\pm 0.01$	0.55 $\pm 0.00$	1.19 $\pm 0.04$	1.55 $\pm 0.01$
Z 5 (2)	12.3 $\pm 0.4$	11.5 $\pm 1.9$	5781 $\pm 4953$	32.5 $\pm 9.5$	75.9 $\pm 25.1$	7.2 $\pm 2.5$	30.3 $\pm 10.0$	6.5 $\pm 2.2$	2.0 $\pm 0.8$	5.8 $\pm 2.0$	1.1 $\pm 0.3$	6.3 $\pm 2.0$	1.4 $\pm 0.4$	3.8 $\pm 1.2$	0.6 $\pm 0.2$	3.1 $\pm 0.8$	0.4 $\pm 0.1$	176.8 $\pm 57.0$	0.73 $\pm 0.04$	0.42 $\pm 0.01$	0.58 $\pm 0.04$	1.10 $\pm 0.03$	1.53 $\pm 0.06$
Z 6 (2)	10.0 $\pm 3.3$	9.6 $\pm 0.6$	7853 $\pm 8294$	40.9 $\pm 18.9$	121.3 $\pm 81.0$	9.2 $\pm 4.6$	43.6 $\pm 25.4$	7.9 $\pm 3.9$	2.5 $\pm 1.2$	7.5 $\pm 3.6$	1.3 $\pm 0.6$	7.4 $\pm 3.1$	1.6 $\pm 0.6$	4.3 $\pm 1.7$	0.6 $\pm 0.2$	3.5 $\pm 1.3$	0.5 $\pm 0.1$	252.2 $\pm 146.2$	0.87 $\pm 0.20$	0.47 $\pm 0.06$	0.55 $\pm 0.06$	1.27 $\pm 0.25$	1.54 $\pm 0.01$
<b>P o s t - m o n s o o n (November and December)</b>																							
Z 0 (2)	10.7 $\pm 1.5$	8.9 $\pm 1.1$	1786 $\pm 58$	28.4 $\pm 0.4$	69.1 $\pm 5.5$	6.6 $\pm 0.1$	28.0 $\pm 0.1$	6.0 $\pm 0.1$	2.0 $\pm 0.0$	5.5 $\pm 0.0$	1.0 $\pm 0.0$	5.9 $\pm 0.1$	1.3 $\pm 0.0$	3.5 $\pm 0.0$	0.5 $\pm 0.0$	2.9 $\pm 0.1$	0.4 $\pm 0.0$	161.0 $\pm 4.9$	0.71 $\pm 0.02$	0.40 $\pm 0.01$	0.56 $\pm 0.00$	1.13 $\pm 0.10$	1.59 $\pm 0.01$
Z 1 (2)	11.1 $\pm 1.9$	10.9 $\pm 2.0$	5563 $\pm 2505$	35.0 $\pm 4.0$	96.2 $\pm 13.8$	7.8 $\pm 0.9$	35.3 $\pm 4.6$	6.9 $\pm 0.7$	2.2 $\pm 0.2$	6.4 $\pm 0.7$	1.1 $\pm 0.1$	6.6 $\pm 0.6$	1.5 $\pm 0.1$	4.0 $\pm 0.4$	0.6 $\pm 0.1$	3.3 $\pm 0.3$	0.5 $\pm 0.0$	207.3 $\pm 26.5$	0.79 $\pm 0.02$	0.45 $\pm 0.01$	0.57 $\pm 0.00$	1.26 $\pm 0.03$	1.57 $\pm 0.01$
Z 2 (2)	10.6 $\pm 0.8$	10.6 $\pm 0.6$	4524 $\pm 430$	34.3 $\pm 0.1$	93.0 $\pm 1.0$	7.6 $\pm 0.2$	34.2 $\pm 0.1$	6.9 $\pm 0.3$	2.2 $\pm 0.1$	6.2 $\pm 0.2$	1.1 $\pm 0.1$	6.6 $\pm 0.3$	1.4 $\pm 0.0$	3.9 $\pm 0.1$	0.6 $\pm 0.0$	3.3 $\pm 0.1$	0.5 $\pm 0.0$	201.7 $\pm 0.4$	0.78 $\pm 0.02$	0.45 $\pm 0.02$	0.57 $\pm 0.01$	1.25 $\pm 0.02$	1.57 $\pm 0.01$
Z 3 (2)	10.1 $\pm 1.2$	9.1 $\pm 1.1$	3325 $\pm 645$	28.3 $\pm 5.0$	72.3 $\pm 8.5$	6.3 $\pm 1.1$	27.6 $\pm 4.2$	5.6 $\pm 1.0$	1.8 $\pm 0.3$	5.1 $\pm 0.9$	0.9 $\pm 0.2$	5.3 $\pm 1.0$	1.2 $\pm 0.2$	3.2 $\pm 0.6$	0.5 $\pm 0.1$	2.6 $\pm 0.5$	0.4 $\pm 0.1$	160.9 $\pm 23.8$	0.79 $\pm 0.03$	0.44 $\pm 0.01$	0.56 $\pm 0.00$	1.19 $\pm 0.06$	1.54 $\pm 0.02$
Z 4 (2)	11.1 $\pm 1.0$	9.9 $\pm 0.3$	3350 $\pm 1997$	29.3 $\pm 6.2$	77.0 $\pm 26.9$	6.6 $\pm 1.5$	29.3 $\pm 7.7$	5.8 $\pm 1.5$	1.8 $\pm 0.5$	5.3 $\pm 1.3$	0.9 $\pm 0.2$	5.5 $\pm 1.3$	1.2 $\pm 0.3$	3.4 $\pm 0.8$	0.5 $\pm 0.1$	2.7 $\pm 0.6$	0.4 $\pm 0.1$	169.7 $\pm 49.0$	0.77 $\pm 0.05$	0.45 $\pm 0.01$	0.58 $\pm 0.03$	1.19 $\pm 0.15$	1.55 $\pm 0.01$
Z 5 (2)	10.5 $\pm 1.0$	10.5 $\pm 0.4$	10044 $\pm 10665$	32.6 $\pm 3.5$	91.0 $\pm 19.2$	7.2 $\pm 0.7$	32.9 $\pm 5.0$	6.4 $\pm 0.6$	2.0 $\pm 0.2$	5.9 $\pm 0.6$	1.0 $\pm 0.1$	6.1 $\pm 0.7$	1.3 $\pm 0.1$	3.7 $\pm 0.4$	0.5 $\pm 0.1$	3.0 $\pm 0.3$	0.4 $\pm 0.0$	194.2 $\pm 31.5$	0.81 $\pm 0.05$	0.46 $\pm 0.02$	0.57 $\pm 0.01$	1.28 $\pm 0.11$	1.56 $\pm 0.01$
Z 6 (2)	10.7 $\pm 2.0$	11.3 $\pm 2.0$	10908 $\pm 4864$	41.7 $\pm 1.2$	123.6 $\pm 6.6$	9.3 $\pm 0.0$	43.9 $\pm 0.9$	8.1 $\pm 0.1$	2.6 $\pm 0.0$	7.5 $\pm 0.1$	1.3 $\pm 0.0$	7.7 $\pm 0.0$	1.7 $\pm 0.1$	4.7 $\pm 0.0$	0.7 $\pm 0.1$	3.8 $\pm 0.0$	0.5 $\pm 0.0$	257.0 $\pm 6.3$	0.86 $\pm 0.04$	0.47 $\pm 0.01$	0.55 $\pm 0.02$	1.34 $\pm 0.08$	1.56 $\pm 0.01$

Table. 4 (Continued)

Stns	Al	Fe	Mn	La	Ce	Pr	Nd	Sm	Eu	Gd	Tb	Dy	Ho	Er	Tm	Yb	Lu	$\sum \text{REE}(\text{L}/\text{H})_n$	$(\text{L}/\text{M})_n$	$(\text{H}/\text{M})_n$	$\text{Ce}/\overset{\circ}{\text{Ce}}$	$\text{Eu}/\overset{\circ}{\text{Eu}}$	
<b>P o s t - m o n s o o n (continued)</b>																							
Z 7 (2)	10.4 ±1.7	10.4 ±2.2	16918 ±7838	35.9 ±4.6	110.8 ±26.3	8.2 ±1.2	38.5 7.3	7.3 ±1.0	2.2 ±0.3	6.6 ±0.9	1.1 ±0.1	6.7 ±0.8	1.5 ±0.2	4.0 ±0.6	0.6 ±0.1	3.3 ±0.5	0.5 ±0.1	227.1 43.9	0.87 ±0.03	0.48 ±0.02	0.55 ±0.01	1.38 ±0.12	1.48 ±0.02
Z 8 (2)	10.8 ±1.0	10.3 ±2.7	3009 ±888	30.0 ±3.7	69.5 ±25.4	6.4 ±1.2	27.4 6.8	5.7 ±1.2	1.7 ±0.4	5.1 ±1.0	0.9 ±0.2	5.4 ±1.0	1.2 ±0.2	3.3 ±0.6	0.5 ±0.1	2.9 ±0.4	0.4 ±0.0	160.6 42.1	0.72 ±0.07	0.44 ±0.01	0.61 ±0.04	1.08 ±0.22	1.49 ±0.07
Z 9 (2)	11.8 ±1.7	13.3 ±0.2	2662 ±657	32.6 ±6.0	89.2 ±18.2	7.0 ±1.1	31.6 6.0	6.3 ±0.9	1.9 ±0.3	5.6 ±0.8	1.0 ±0.1	6.0 ±0.8	1.3 ±0.1	3.7 ±0.4	0.6 ±0.1	3.2 ±0.3	0.5 ±0.0	190.5 35.1	0.75 ±0.07	0.46 ±0.03	0.62 ±0.02	1.27 ±0.03	1.49 ±0.00
<b>P r e - m o n s o o n (March and May)</b>																							
Z 0 (1)	10.0	8.6	1795	30.7	76.5	7.0	29.8	6.4	2.1	5.8	1.0	6.2	1.4	3.7	0.6	3.1	0.4	174.8	0.72	0.41	0.57	1.16	1.63
Z 1 (2)	9.3 ±1.2	9.3 ±1.2	5956 ±1634	33.3 ±8.9	103.7 ±33.5	7.6 ±2.0	35.8 ±10.5	6.8 ±1.8	2.2 ±0.6	6.2 ±1.6	1.1 ±0.3	6.4 ±1.7	1.4 ±0.3	3.8 ±1.0	0.5 ±0.1	3.1 ±0.7	0.4 ±0.1	212.2 62.9	0.86 ±0.04	0.47 ±0.02	0.55 ±0.01	1.39 ±0.07	1.56 ±0.00
Z 2 (2)	9.6 ±0.4	9.3 ±0.7	4421 ±806	30.1 ±4.4	85.9 ±12.9	6.7 ±0.9	30.4 4.4	6.1 ±0.8	1.9 ±0.3	5.5 ±0.8	1.0 ±0.1	5.7 ±0.8	1.2 ±0.2	3.5 ±0.5	0.5 ±0.1	2.8 ±0.4	0.4 ±0.1	181.8 26.5	0.81 ±0.01	0.45 ±0.00	0.56 ±0.00	1.31 ±0.01	1.57 ±0.01
Z 3 (2)	7.4 ±1.0	6.2 ±2.2	2879 ±3234	19.2 ±9.1	49.9 ±31.6	4.4 ±2.1	18.8 ±10.0	3.9 ±1.9	1.2 ±0.6	3.4 ±1.8	0.6 ±0.3	3.6 ±1.8	0.8 ±0.4	2.2 ±1.1	0.3 ±0.2	1.8 ±0.8	0.3 ±0.1	110.4 61.7	0.75 ±0.06	0.44 ±0.02	0.58 ±0.02	1.16 ±0.19	1.55 ±0.02
Z 4 (2)	10.2 ±0.4	9.9 ±0.9	5271 ±940	31.2 ±5.7	89.5 ±24.8	7.0 ±1.3	31.8 8.1	6.3 ±1.1	2.0 ±0.4	5.7 ±1.1	1.0 ±0.2	5.8 ±1.0	1.3 ±0.2	3.5 ±0.5	0.5 ±0.1	2.9 ±0.5	0.4 ±0.0	188.7 45.0	0.82 ±0.07	0.46 ±0.02	0.56 ±0.01	1.30 ±0.09	1.55 ±0.02
Z 5 (2)	9.8 ±1.4	11.7 ±1.5	20282 ±20922	53.1 ±31.2	159.2 ±99.4	10.8 ±5.5	53.2 ±31.4	9.4 ±4.7	3.0 ±1.5	8.8 ±4.6	1.5 ±0.7	8.5 ±4.0	1.9 ±0.9	5.0 ±2.2	0.7 ±0.3	4.0 ±1.7	0.5 ±0.1	319.6 188.1	0.97 ±0.21	0.50 ±0.05	0.53 ±0.06	1.36 ±0.06	1.54 ±0.02
Z 6 (2)	10.3 ±0.5	10.4 ±0.1	6709 ±289	35.9 ±0.8	102.2 ±11.1	8.2 ±0.2	38.4 ±0.2	7.3 ±0.1	2.3 ±0.1	6.9 ±0.4	1.2 ±0.1	6.9 ±0.2	1.6 ±0.1	4.3 ±0.4	0.6 ±0.0	3.3 ±0.0	0.5 ±0.1	219.5 11.0	0.81 ±0.08	0.45 ±0.04	0.55 ±0.01	1.28 ±0.12	1.54 ±0.00
Z 7 (2)	9.9 ±0.1	11.2 ±1.4	27951 ±24719	40.8 ±9.2	146.8 ±54.6	9.3 ±2.4	47.9 ±16.2	8.4 ±2.4	2.6 ±0.7	7.8 ±2.5	1.3 ±0.4	7.8 ±2.3	1.7 ±0.5	4.7 ±1.4	0.7 ±0.2	3.7 ±1.0	0.5 ±0.1	284.0 93.8	0.93 ±0.05	0.50 ±0.01	0.54 ±0.02	1.54 ±0.16	1.50 ±0.02
Z 8 (2)	10.3 ±0.2	12.0 ±1.0	10183 ±11404	32.6 ±8.2	101.5 ±41.5	7.1 ±2.1	33.8 ±12.3	6.2 ±1.9	1.8 ±0.4	5.5 ±1.6	1.0 ±0.2	5.6 ±1.2	1.2 ±0.3	3.4 ±0.7	0.5 ±0.1	2.9 ±0.5	0.4 ±0.1	203.5 71.1	0.88 ±0.13	0.51 ±0.05	0.58 ±0.04	1.39 ±0.17	1.46 ±0.08
Z 9 (2)	7.0 ±8.1	8.1 ±9.0	3827 ±3132	28.3 ±6.9	77.8 ±18.9	6.2 ±1.2	28.1 ±4.6	5.5 ±0.8	1.6 ±0.3	4.8 ±0.7	0.9 ±0.1	4.9 ±0.8	1.1 ±0.2	3.1 ±0.4	0.5 ±0.1	2.6 ±0.4	0.4 ±0.1	165.7 35.5	0.80 ±0.05	0.48 ±0.02	0.60 ±0.01	1.26 ±0.04	1.48 ±0.05

The number in brackets in the first column indicates the number of samples analyzed at each station.

Table.5 Concentrations of Al (%), Fe (%), Mn ( $\mu\text{g/g}$ ) and REEs ( $\mu\text{g/g}$ ) in surface sediments on the continental shelf off Zuari estuary.

Stns	Depth (m)	Al	Fe	Mn	La	Ce	Pr	Nd	Sm	Eu	Gd	Tb	Dy	Ho	Er	Tm	Yb	Lu	$\Sigma\text{REE}$	$(\text{L/H})_n$	$(\text{L/M})_n$	$(\text{H/M})_n$	$\text{Ce}^*/\text{Ce}$	$\text{Eu}^*/\text{Eu}$
S1	7	11.5	7.8	430	31.4	80.2	7.3	30.2	6.7	2.2	6.0	1.1	6.5	1.4	3.8	0.6	3.1	0.4	180.8	0.74	0.61	0.83	1.22	1.61
S2	7	11.0	9.4	2538	32.7	86.1	7.5	31.9	6.8	2.2	6.1	1.1	6.3	1.4	3.9	0.5	3.0	0.4	189.9	0.78	0.64	0.82	1.27	1.60
S3	11	10.8	9.1	1217	28.4	72.8	6.4	27.5	6.0	1.9	5.4	1.0	5.7	1.2	3.4	0.5	2.7	0.4	163.4	0.75	0.62	0.83	1.24	1.60
S4	15	10.9	8.8	1000	24.2	56.9	5.5	23.0	5.0	1.6	4.6	0.8	4.7	1.0	2.8	0.4	2.3	0.4	133.4	0.73	0.61	0.85	1.13	1.56
S5	18	10.7	9.0	575	29.3	74.5	6.7	29.1	6.2	2.1	5.8	1.0	6.1	1.3	3.7	0.5	2.9	0.4	169.8	0.72	0.60	0.83	1.22	1.62
S6	14	11.4	7.9	327	18.6	41.1	4.3	17.9	3.9	1.2	3.6	0.6	3.8	0.8	2.2	0.3	1.9	0.3	100.6	0.69	0.60	0.88	1.06	1.55
S7	11	10.3	7.2	390	12.5	25.6	2.8	11.4	2.4	0.7	2.2	0.4	2.3	0.5	1.4	0.2	1.2	0.2	63.9	0.66	0.64	0.97	0.99	1.47
S8	19	10.8	9.1	511	28.5	74.6	6.8	28.3	6.1	2.1	5.7	1.0	6.1	1.3	3.6	0.5	2.9	0.4	167.9	0.72	0.60	0.83	1.24	1.64
S9	19	11.1	9.1	487	27.9	70.7	6.5	27.2	5.9	1.9	5.5	1.0	5.9	1.3	3.5	0.5	2.8	0.4	161.1	0.70	0.60	0.85	1.22	1.58
S10	32	10.7	8.6	498	26.7	68.8	6.2	26.0	5.6	1.8	5.2	0.9	5.6	1.2	3.3	0.5	2.7	0.4	154.9	0.72	0.61	0.85	1.23	1.61
S11	20	10.7	9.0	509	30.4	78.9	7.0	30.0	6.5	2.2	6.0	1.1	6.4	1.4	3.8	0.6	3.0	0.4	177.8	0.72	0.60	0.84	1.24	1.62
S12	23	10.9	9.0	669	27.7	71.7	6.3	27.2	5.9	1.9	5.3	1.0	5.7	1.2	3.4	0.5	2.7	0.4	161.1	0.72	0.61	0.85	1.25	1.62
S13	34	11.3	8.7	536	23.3	51.2	5.4	22.2	4.9	1.6	4.4	0.8	4.8	1.0	2.8	0.4	2.3	0.3	125.4	0.70	0.59	0.85	1.06	1.58
S14	22	11.1	9.3	669	23.7	53.3	5.4	22.6	5.0	1.6	4.5	0.8	4.8	1.0	2.8	0.4	2.4	0.4	128.8	0.70	0.60	0.86	1.08	1.57
S15	18	10.9	9.4	745	26.0	67.6	6.1	25.2	5.5	1.8	4.9	0.9	5.2	1.2	3.1	0.5	2.6	0.4	150.9	0.73	0.62	0.85	1.24	1.62
S16	34	10.9	9.2	617	29.4	76.6	6.8	28.5	6.2	2.0	5.6	1.0	6.1	1.3	3.7	0.5	2.9	0.4	171.1	0.73	0.62	0.85	1.25	1.60
S17	45	9.8	7.8	343	24.5	55.2	5.7	23.5	5.1	1.6	4.7	0.8	4.9	1.1	3.0	0.4	2.5	0.4	133.3	0.69	0.60	0.87	1.08	1.54
S18	54	9.4	7.7	361	23.0	56.6	5.4	22.5	4.9	1.6	4.4	0.8	4.9	1.1	2.9	0.4	2.4	0.3	131.1	0.70	0.61	0.87	1.17	1.58
S19	102	6.2	4.6	218	14.4	27.4	3.2	12.7	2.8	0.8	2.6	0.5	2.9	0.7	1.9	0.3	1.6	0.2	72.1	0.59	0.58	0.98	0.92	1.44
S20	200	4.9	3.4	176	13.0	23.6	2.8	10.9	2.4	0.7	2.2	0.4	2.4	0.5	1.6	0.2	1.3	0.2	62.1	0.63	0.62	0.98	0.89	1.38